R. & M. No. 2935
(15,633)
A.R.C. Technical Report

F.

MINISTRY OF SUPPLY

AERONAUTICAL RESEARCH COUNCIL
REPORTS AND MEMORANDA

Card

A Simple Method for Calculating the Span and Chordwise Loading on Straight and Swept Wings of any Given Aspect Ratio at Subsonic Speeds

By

D. KÜCHEMANN, Dr.rer.nat.

LONDON: HER MAJESTY'S STATIONERY OFFICE
1956

PRICE 13*s* 6*d* NET

A Simple Method for Calculating the Span and Chordwise Loading on Straight and Swept Wings of any Given Aspect Ratio at Subsonic Speeds

By

D. KÜCHEMANN, Dr.rer.nat.

COMMUNICATED BY THE PRINCIPAL DIRECTOR OF SCIENTIFIC RESEARCH (AIR), MINISTRY OF SUPPLY

Pe

LO

Reports and Memoranda No. 2935*

August, 1952

Summary.—The methods of classical aerofoil theory are used to derive a general theory for wings of any given plan form. Accordingly, the general downwash equation is split into two parts: one, the effective incidence, being due to the downwash induced by the vorticity component along the span; and the other, the induced incidence, which is due to the downwash induced by the streamwise vorticity component. The latter is related to the downwash in the Trefftz plane, and a downwash factor is introduced to include both the limiting cases of very small aspect ratio (Jones) and of very large aspect ratio (Prandtl). The downwash resulting from the spanwise vortices is approximated by a simple relation, the accuracy of which is proved to be satisfactory for practical purposes, and an exact solution of this equation is given for wings of very large aspect ratio, swept or unswept. For wings of moderate or small aspect ratios, the solution given fulfills the approximate downwash equation only in the mean over the whole chord, *i.e.*, the downwash is correct not at a few discrete points but on the average. Again, the limiting cases of Jones and Prandtl are included in the present solution. Thus, the load over the whole surface of a given wing can be calculated at a given subcritical Mach number, and the procedure is as simple and rapid as that of the classical aerofoil theory. The calculated results are confirmed by experiment.

With this method, the effects of wing thickness and of the boundary layer can easily be taken into account, as well as aero-elastic effects. Non-linearity of the lift due to tip vortices is also treated.

LIST OF SYMBOLS

x, y, z	Rectangular co-ordinates; $x = 0$ at leading edge; x positive in the direction of the main stream; x, y, z are measured in terms of the wing chord if not specifically stated otherwise
c	Wing chord
$\bar{c}$	Mean wing chord
b	Wing span
t	Wing thickness
h	Height of tip vortex

* R.A.E. Report Aero. 2476, received 13th February, 1953.

$x_{\text{a.c.}}$		Chordwise position of the aerodynamic centre
η	=	$2y/b$ (or $2yc/b$)
A	=	$b/\bar{c}$; aspect ratio
α		Geometric angle of incidence
α_0		Zero lift angle
α_e		Effective angle of incidence
α_{e0}		Effective angle of incidence on swept wing of large aspect ratio
α_{ep}		Effective incidence on two-dimensional wing in inviscid flow
δ	=	α_{ep}/α_e
α_i		Induced angle of incidence
α_{i0}		Induced angle of incidence on wings of large aspect ratio
φ		Angle of sweep of mid-chord line
φ_e		Effective angle of sweep, equation (86)
φ_v		Angle of sweep of vorticity vector
V_0		Velocity of the main stream
v_z		Induced velocity in z-direction
v_{z0}		Induced velocity on swept wing of large aspect ratio
Γ		Strength of spanwise vortices
$\gamma_x(x)$		Distribution of spanwise vortices along the chord
γ	=	$\Gamma/bV_0 = C_L c/2b$; non-dimensional vortex distribution
ΔC_p		Difference of the pressure coefficients on upper and lower surfaces of the wing
C_N		Normal force coefficient of section
C_T		Tangential force coefficient of section
C_L		Lift coefficient of section
C_D		Drag coefficient of section
C_m		Pitching moment coefficient of section
$\bar{C}_L$		Overall lift coefficient of wing
a_0		Lift slope coefficient of two-dimensional aerofoil
a	=	C_L/α_e ; sectional lift slope coefficient
n		Number between 0 and 1, dependent on A, φ, and y
n_0		Value of n on swept wing of large aspect ratio
σ	=	$\pi \cot \pi n_0$
ω		Downwash factor, between 1 and 2, dependent on A and φ
λ		Interpolation function, Fig. 23
M_0		Free-stream Mach number
β	=	$\sqrt{(1 - M_0^2)}$

Suffixes :

s	Sheared part of the wing
c	Centre of swept wing
T	Tip of swept wing
a	Analogous wing

1. *Introduction.*—The purpose of the present report is to provide a method for calculating the load over the surface of a thin wing of any given plan form, which is suitable for practical application in the design of high-speed, subsonic aircraft. To be of use, such a method must be simple enough to be performed in a few hours by a computer, and it must be applicable to wings of any taper and sweep and to aspect ratios down to about one. It is also essential that the method can easily be extended to cambered wings, cranked wings, and to wings with fuselage or with other bodies attached to it, and also to elastic wings*. Such a method should also provide the basis for calculating the pressure distribution on the surface of wings of non-zero thickness and for estimating the effect of the boundary layer on the lift and pressure distribution†. The application to compressible subsonic flow should not necessitate the use of 'rules' which are based on two-dimensional flow conditions but enable the load on the given, three-dimensional, wing to be computed at a given subcritical Mach number. With the complete method at his disposal, the designer should be able to choose wing plan form, camber and twist, section shape and fuselage contours so as to obtain the best compromise to meet his requirements.

The present report deals with part of the general problem, namely, the load on thin uncambered wings. Use is made of existing methods which are valid in the following limiting cases:

(*a*) The classical aerofoil theory of L. Prandtl[1] for unswept wings of very large aspect ratio (above 6, say), and for sheared wings of infinite span.

(*b*) The theory of R. T. Jones[2] for straight and swept wings of very small aspect ratio (below about 0·5).

(*c*) The theory of Ref. 3 for swept wings of large aspect ratio (above about 3).

Nearly all practical wings without sweep, and many swept wings, fall in the aspect ratio range between these limiting cases, and the aim of the method presented here is to be applicable to this intermediate range of aspect ratio and, at the same time, to fulfil the requirements set out above. Since an investigation of a wing in compressible subsonic flow usually means treating an analogous wing of smaller aspect ratio than the original, some emphasis is put here on the effects associated with small aspect ratio.

The three limiting theories are fundamentally similar to each other in that the span loading is obtained from the same type of integral equation as that which occurs in the classical aerofoil theory. This type of equation is, therefore, assumed to hold also in the intermediate cases which thus retain the simplicity and advantages of the classical aerofoil theory. The induced downwash on the wing surface is then always considered in two parts: the 'effective incidence', α_e, which is related to the spanwise vortex component; and the 'induced incidence', α_i, which is related to the streamwise vortex component, consisting mainly of trailing vortices. Further, a certain type of chordwise loading which is characterised by a single shape parameter, n, is common to all the limiting theories. This type of chordwise loading is, therefore, assumed to hold also in the intermediate cases. The shape parameter n depends mainly on the aspect ratio of the wing and can be related to the effective incidence and the induced incidence. In determining these relations, use is again made of the results obtained in the limiting cases.

The present method is different from current theoretical work on the subsonic flow past three-dimensional aerofoils, which is characterised by efforts to solve the problem by more mathematical methods, the use of physical concepts being on the whole limited to the basic equations of motion. This procedure is necessarily complicated, and an application to the practical problems mentioned above is not normally possible. Since the methods so far available always involve simplifications (even in the numerical evaluation, such as restrictions in the number of terms in series), none of

* Cambered wings are treated on the basis of the present method in Ref. 4, cranked wings in Ref. 5, wings with fuselage in Ref. 6, wings with tip tanks in Ref. 7, and fin-body combinations in Ref. 8. B. A. Hunn[9] has shown how a method like the present one can be adapted to calculate elastic wings.

† Wings of non-zero thickness are treated in relation to the present method in Ref. 10, and the effects of the boundary layer, for a simple case, in Ref. 11.

the solutions obtained are exact enough to be considered as a standard against which the present method could be checked. In general, the only means of checking is by experiment. There are, however, a number of special cases which have been treated by means of a formidable mathematical apparatus. Comparison between the results obtained in those cases and the results of the present method give very good agreement. This appears to show that the approach used here takes adequate account of all the main factors involved, in spite of its simplicity.

The report is divided into two parts, the first dealing with unswept wings and the second with swept wings. To clarify the present approach, Prandtl's classical aerofoil theory will be re-interpreted and the similarities to Jones's method demonstrated. At the same time, the meaning of the terms ' lifting-line ' theory and ' lifting-surface ' theory, as used here, will be more clearly defined, the present method representing essentially a lifting-surface theory. It will be shown that methods based on the concept of a lifting line and the three-quarter chord theorem cannot be justified. Non-linear lift effects will be considered and, finally, the method will be applied to compressible flow at subcritical Mach numbers by means of the Prandtl-Glauert analogy. The purpose of the present report is to derive and explain the theoretical basis of the calculation method. A more detailed description of the calculation procedure will be given in a later note, in which the practical application of the methods of Refs. 4 to 8, and 10, 11 will also be explained, together with worked examples.

2. *Straight Wings*.—The theory will first be developed for unswept wings. These are assumed to have no appreciable kinks in either leading or trailing edge, the mid-chord line being roughly at right-angles to the direction of the main stream.

2.1. *Re-interpretation of Prandtl's Aerofoil Theory*.—Consider a plane unswept wing. As a lifting surface, the wing is replaced by a system of vortices* situated partly on the wing (bound vortices) and partly left behind in the free stream (free vortices). If the wing is symmetrical about the x-axis, as in Fig. 1, the bound vortices will cross the centre-line at right-angles. Elsewhere on the wing they are curved and neither parallel to the y-axis nor to the x-axis. The foremost vortex runs parallel to the leading edge. When leaving the wing, the vortices ought to cross the trailing edge at right-angles to avoid a vorticity component parallel to the trailing edge; otherwise, the Kutta condition of smooth flow from the trailing edge would not be fulfilled†.

The strength and direction of the vorticity vector at any point on the wing surface is determined by the streamline condition, *i.e.*, the resultant of the free-stream velocity, V_0 and that induced by the vortex system, v_z, must be parallel to the wing surface. For a thin flat wing at incidence α,

$$\frac{v_z(x, y)}{V_0} = \frac{dz\,(x, y)}{dx} = \alpha = \text{const.} \qquad \ldots \qquad (1)$$

everywhere. The induced velocity v_z is obtained by integrating the contributions of the individual vortex elements over the wing surface and the wake. The velocity induced by a vortex element is given by the Biot-Savart law. If the strength and direction of the vorticity vector at every point are known, the velocity field, and hence the forces on the wing can be determined.

In view of the complexity of the problem of finding the unknown vorticity distribution from a double integral equation of the first kind, it is not surprising that so far no exact solution is known. The theoretical treatment here is, therefore based on physically plausible assumptions. In the following, Prandtl's treatment of this problem will be interpreted in a way which readily allows it to be extended subsequently to wings of arbitrary plan form.

---

* We prefer to retain the concept of vortices because of its obvious physical interpretation and because their behaviour is governed by well-known theorems. The argument can, of course, be developed also in terms of a pressure potential (since $\Delta C_p = -2\gamma_z/V_0$), or in terms of the specific enthalpy of the flow (since $\Delta i = -V_0\gamma_z$), if one so desires.

† This is, of course, generally ignored in any linearised theory, the free vortices being assumed to lie along the main stream everywhere.

The bound vorticity vector at any point is resolved into a component γ_x parallel to the spanwise co-ordinate y and a component ε_b parallel to the chordwise co-ordinate x. The former will be called the 'spanwise vortex component'; the latter the 'chordwise vortex component'. Behind the wing, the chordwise vortices are continued by the trailing vortices, ε_w. The configuration of the vortices, as illustrated in Fig. 1, is essentially similar for both large and small aspect ratio.

The problem of calculating the downwash v_z may be greatly simplified by considering the downwash, v_{z1}, induced by the spanwise vortices γ_x separately from the downwash, v_{z2}, induced by the streamwise vortices ε_b and ε_w. The sum of the two contributions must be constant across the chord :—

$$v_{z1}(x) + v_{z2}(x) = v_z = \alpha V_0$$

by equation (1). The mean value

$$\frac{1}{V_0}\int_0^1 v_{z1}(x)\,dx = \alpha_e \quad \ldots \quad (2)$$

may be described as the 'effective incidence' of the aerofoil; and the mean value

$$\frac{1}{V_0}\int_0^1 v_{z2}(x)\,dx = \alpha_i \quad \ldots \quad (3)$$

as the 'induced incidence.' The boundary condition (1) can then be replaced by the weaker condition $\alpha = \alpha_e + \alpha_i$.

The next step is to relate α_e to the distribution of the spanwise vortices. These are straight but their strength varies along the span. They are of finite length, lying within the wing span. Here Prandtl introduces what may now be formulated as the hypothesis that the downwash v_{z1} induced by these at any spanwise station is, to a first approximation, the same as the downwash v_{z0} induced by vortices having the same direction and chordwise distribution as those at the station but of infinite length at either side of it. The fact that the spanwise vortices are of finite length and that their strength varies is thus ignored. This hypothesis is obviously justified for wings of large aspect ratio, with the exception of their tip regions where it cannot be strictly true. Near the tips, the vortex lines are necessarily curved (*see* Fig. 1) and the 'small aspect ratio' effects, which will be discussed below, must therefore be expected in the tip regions of wings of very large aspect ratio; for instance, the position of the aerodynamic centre moves forward as the tip is approached. However, the tips contribute little to the overall lift of the wing and no great error is involved to the overall result by applying Prandtl's hypothesis to the whole span.

For a vortex distribution $\gamma_x(x)$ of infinite length,

$$\frac{v_{z1}}{V_0} = \frac{v_{z0}}{V_0} = \frac{1}{2\pi V_0}\int_0^1 \gamma_x(x')\,\frac{dx'}{x - x'} \quad \ldots \quad (4)$$

by Biot-Savart's law. If we take $\gamma_x(x)$ to be the 'flat-plate' distribution of Birnbaum[12],

$$\gamma_x(x) = C\left(\frac{1-x}{x}\right)^{1/2},$$

then

$$\frac{v_{z1}}{V_0} = \frac{1}{2\pi V_0}\,C\pi = \frac{C}{2V_0},$$

i.e., v_{z1} is independent of x, and $\alpha_e = C/2V_0$ by equation (2). The constant C can be related to the sectional lift coefficient. At any point, x, along the chord, the flow is inclined at an angle

α_e to the chord line and the velocity of the flow is $V_0 \cos \alpha_e \simeq V_0$, because α_e is assumed to be small (*see* Fig. 2). The Kutta-Joukowski theorem states that the force $l(x)$ on the vortex element $\gamma_x(x)$ is

$$l(x) = \rho V_0 \gamma_x(x) .$$

This force is normal to the relative wind direction, *see* Fig. 2. Only the spanwise vortices appear in this relation since the streamwise vortices lie along the wind and do not sustain any force. Thus α_e gives the direction in which the resultant air force has no component. The aerofoil experiences this force as a difference, $-\Delta p$, in the pressures on its upper and lower surfaces. Δp is a force normal to the chord-line. Thus $-\Delta p(x) = l(x) \cos \alpha_e \simeq l(x)$, so that

$$-\Delta p(x) = \rho V_0 \gamma_x(x) ,$$

or, non-dimensionally,

$$\Delta C_p(x) = \frac{\Delta p(x)}{\frac{1}{2}\rho V_0^2} = -\frac{2}{V_0} \gamma_x(x) . \qquad (5)$$

The overall lift of the section is obtained by integration :—

$$L = c \int_0^1 l(x)\, dx .$$

Hence,

$$C_L = \frac{L}{\frac{1}{2}\rho V_0^2 c} = -\int_0^1 \Delta C_p(x)\, dx = \frac{2}{V_0} \int_0^1 \gamma_x(x)\, dx . \qquad (6)$$

This gives for the flat-plate distribution

$$C_L = \frac{2}{V_0} C \int_0^1 \left(\frac{1-x}{x}\right)^{1/2} dx = \frac{\pi}{V_0} C ,$$

so that $C = C_L V_0/\pi$, and

$$\gamma_x(x) = \frac{V_0}{\pi} C_L \left(\frac{1-x}{x}\right)^{1/2} ; \qquad \Delta C_p(x) = -\frac{2}{\pi} C_L \left(\frac{1-x}{x}\right)^{1/2} . \qquad (7)$$

Further,

$$\alpha_e = \frac{C}{2V_0} = \frac{C_L}{2\pi} ; \quad \text{or} \quad a = \frac{C_L}{\alpha_e} = 2\pi = a_0 . \qquad (8)$$

This states that the effective incidence is a linear function of the lift coefficient and that the 'two-dimensional lift slope' a_0 has the value 2π for a flat-plate aerofoil*. In the classical aerofoil theory the expression (8) for α_e is assumed to hold at any spanwise station of a wing of finite aspect ratio, although it is derived for and strictly applies only to two-dimensional aerofoils.

To find the induced incidence α_i from the downwash $v_{z\,2}$ of the streamwise vortices by equation (3), we consider first the contribution $\alpha_{i\,0}$ of the trailing vortices. These, starting at the trailing edge, induce a downwash at the trailing edge which is equal to half the downwash induced by them far behind the wing, if the trailing edge is straight and unswept. This value, $\alpha_{i\,0}$, is given by the well-known integral

$$\alpha_{i\,0} = \frac{1}{2\pi} \int_{-1}^{+1} \frac{d\gamma(\eta')}{d\eta'} \frac{d\eta'}{\eta - \eta'} \qquad (9)$$

---

* $a_0 = 2\pi$ only for the two-dimensional flat plate in inviscid flow. For two-dimensional aerofoils on non-zero thickness in viscous flow, $a = a_0 = k(1 + \varepsilon)2\pi$, where ε takes account of the thickness of the aerofoil and can be approximated by $\varepsilon = 0 \cdot 8\, t/c$. k measures the lift reduction due to the boundary layer. $k = 0 \cdot 92$ for RAE 101 section of $t/c = 0 \cdot 10$ at a Reynolds number of about 2×10^6 at zero lift, as explained in Refs. 11 and 13.

where $\eta = 2y/b$ and $\gamma = C_L c/2b$. Prandtl's contention is now that the wing chord is so small compared with the span that the downwash from the trailing vortices does not vary very much along the chord and that the additional effect of the chordwise vortices ε_b is such as to keep the mean value of α_i at the value α_{i0} as given by equation (9), i.e., $\alpha_i = \alpha_{i0}$. This is reasonable for wings of large aspect ratio, again with the exception of the tip regions.

From the boundary condition $\alpha_e = \alpha - \alpha_i$ we find now, from equations (8) and (9),

$$\alpha_e = \frac{C_L}{a_0} = \frac{2b}{a_0 c}\gamma(\eta) = \frac{2A}{a_0 c/\bar{c}}\gamma(\eta) = \alpha - \frac{1}{2\pi}\int_{-1}^{+1}\frac{d\gamma(\eta')}{d\eta'}\,\frac{d\eta'}{\eta - \eta'}, \quad \ldots \quad \ldots \qquad (10)$$

which is the well-known integral equation for the spanwise loading. Having determined $\gamma(\eta)$ and thus $C_L(\eta)$, we find the chordwise loading from equation (7).

The distribution of the various downwash contributions is similar to that shown in Fig. 3*. The lift is produced by the interaction of the main flow, which has the velocity V_0 at an angle α_e with the spanwise vortices, as explained above. The drag is produced by the interaction of the downwash $v_{z\,2}$ from the streamwise vortices with the spanwise vortices, since only the streamwise vortices are associated with the kinetic energy in downward movement of the air far behind the wing. This energy is, in fact, equal to the work done by the drag force experienced by the aerofoil: Since α_e is assumed to be independent of the aspect ratio of the wing, by equation (8), the value of α_i must depend on the aspect ratio, by equations (9) and (10). The relation between the lift and the drag forces on the wing then depends also on the aspect ratio. Resolving the resultant air force into a component, C_N normal to the chord-line and into a component, C_T, tangential to the chord-line, we find from Fig. 2 that $C_T = -C_N\alpha_e$. Since α_e is assumed to be independent of the aspect ratio, the relation between the normal and tangential forces on the wing should not depend on the aspect ratio†. In fact, $C_T = -C_N^2/2\pi = -C_N^2/a_0$ by equation (8), since $C_N \simeq C_L$.

Whether this is sufficiently correct in practice can easily be checked by experiment. It is found that a quadratic relation between C_N and C_T is indeed fulfilled with remarkable accuracy, as can be seen from the examples‡ in Fig. 5. The fact that the lines are straight shows that it is reasonable to use the concept of the effective incidence. As the results for wings of large aspect ratio (from about 6 upwards) fall together, it follows that the effective incidence and the sectional lift slope can be adequately determined from the properties of the two-dimensional aerofoil. In this case the slope of the C_N^2 vs. C_T lines is $-1/a_0$, where a_0 is the two-dimensional lift slope, and it follows that the chordwise loading is given by the two-dimensional distribution with sufficient accuracy.

However, it can be seen from Fig. 5 that only the results from wings with large aspect ratio fall together, the lines becoming gradually steeper as the aspect ratio decreases. This indicates the limitations of Prandtl's aerofoil theory in its original form. An extension of this theory is obviously needed. In extending the theory, it does not seem necessary to abandon the concepts of the effective incidence and of a sectional lift slope which is independent of the geometric incidence since the C_N^2 vs. C_T lines are still straight. However, there must be a redistribution of the spanwise vortices along the chord, for only this will give a sectional lift slope which decreases with aspect ratio and thus different slopes of the C_N^2 vs. C_T lines. This, then, is the basic approach which will be used below.

---

* Fig. 3 is not drawn to scale, and the lines representing the variations along the chord of the individual contributions are entirely arbitrary.

† Another derivation of this relation is given in Ref. 14.

‡ These tests[15] were made with cambered aerofoils, where

$$C_T = -C_N^2/a - C_N\alpha_0$$

as shown in Ref. 14. α_0 is the zero-lift angle of the two-dimensional cambered aerofoil.

It may be noted that such a simple relation as $C_T = -C_N^2/a$ is not used in any of the mathematical lifting-surface theories, simply because the concepts of the effective incidence and of the sectional lift slope are not introduced. However, the fact that $a = -C_N^2/C_T$ has a constant value which is independent of the incidence is implicit in such theories, as can readily be seen from the Kutta-Joukowski theorem under the assumptions of linearised theory. The tangential force is obtained by integrating along the chord the product of density, ρ, vortex strength, $\gamma_x(x)$, and downwash, $z_{z1}(x)$. According to linearised theory, both γ_x and v_{z1} (and $v_{z2} = v_z - v_{z1}$ for that matter) are proportional to the incidence α. Hence, C_T is proportional to C_N^2 which leads directly to $a = C_L/\alpha_e$ if α_e is defined as $\alpha_e = -C_T/C_N$, as above.

The classical aerofoil theory of Prandtl is often described as a ' lifting-line ' theory, in contrast to ' lifting-surface ' theories. It will be noted, however, that it is quite unnecessary in the present derivation to introduce the concept of a lifting line on which all the circulation of the spanwise vortices is concentrated. Indeed, this concept could only be used to derive the relation for α_i ($= \alpha_{i0}$ from equation (9)). But this relation is just as easily obtained from the assumption that the chord is small compared with the wing span*, as there is still a well-defined chord-wise distribution of vortices, namely that of the two-dimensional flat plate, however small the chord is. The assumption of a chordwise distribution of vortices, on the other hand, is essential for determining the sectional lift slope, which cannot otherwise be obtained. It certainly does not follow from the assumption of a lifting line. Obviously, the term lifting-line theory has been loosely applied, and it is proposed to use it only in such cases where a theory is truly based and developed on the assumption that the spanwise vortices are concentrated in one, or several, discrete vortex filaments. It is proposed to use the term ' lifting-surface theory ' to describe any method where a distribution of spanwise and streamwise vortices (or of any other singularities) over the whole wing surface is considered. In this sense, Prandtl's classical aerofoil theory is a lifting-surface theory, limited, however, to wings of large aspect ratio. A clarification of these concepts is particularly desirable since the literal application of the concept of the lifting line to refining the classical aerofoil theory, and to extending it to swept wings, has not proved successful. This in turn has brought some unjustified discredit to the basic approach of Prandtl. It will be shown below that the basic concepts of the classical aerofoil theory can successfully be used for obtaining a method which is satisfactory throughout the whole aspect ratio range.

There are certain similarities in the basic concepts between Prandtl's theory and R. T. Jones's theory[2] for wings of very small aspect ratio. It is found that the chordwise loading is different from that of the two-dimensional aerofoil in that the lift concentrates nearer to the leading edge as $A \to 0$. In the limit as $A \to 0$, the effective incidence induced by the spanwise vortices tends to zero, leaving only the chordwise and the trailing vortices to fulfil the boundary condition: $\alpha = \alpha_i$ for $\alpha_e = 0$, in contrast to the two-dimensional aerofoil where $\alpha = \alpha_e$ because $\alpha_i = 0$. As the downwash from the spanwise vortices decreases, the chordwise vortices grow longer compared with the wing span and the downwash induced by them increases. In the limit $A = 0$, their effect is such as to keep the mean value of α_i at the value $2 \times \alpha_{i0}$ as given by equation (9), *i.e.*, twice the value for wings of very large aspect ratio. This implies that the flow in planes $x =$ const can be considered as being two-dimensional, the chordwise and trailing vortices together being effectively of infinite length on either side of the section considered, instead of semi-infinite length as for high aspect ratio wings. For the present purpose, it is important to note that the span loading is again obtained from an equation of the same type as Prandtl's equation, equation (10), the left-hand side being zero and the downwash integral having a factor 2.

2.2. *Exposition of the New Method.*—In order to treat wings in the practical range of aspect ratios between the limiting cases of Jones and Prandtl, we shall first of all show that it is reasonable to retain the concepts of an effective incidence and of a sectional lift slope, *i.e.*, to treat the effect of the spanwise vortices separately from that of the chordwise and trailing

* *See* also the analytical derivation given by H. R. Lawrence[16].

vortices. This can readily be seen from experiments such as those plotted in Fig. 5. We find that C_N and C_T, which depend on the chordwise distribution of the spanwise vortices only, obey the relation $C_T = - C_N^2/a$ throughout the whole aspect ratio range tested. This implies that it is still reasonable to use an effective incidence, as in Fig. 2, and that the relation $C_L = a\alpha_e$ holds throughout the whole range, the value of a being independent of incidence for each aspect ratio but varying with aspect ratio. This follows also from the Kutta-Joukowski theorem under the assumptions of linearised theory as shown above (the derivation applies to any section on any wing of any given aspect ratio) and is thus tacitly implied in any existing theory.

On this basis we may proceed to determine the value of a. This will be done by using the hypothesis from above which leads to

$$\alpha_e = \int_0^1 \frac{v_{z1}}{V_0}\, dx = \frac{1}{2\pi V_0} \int_0^1 \int_0^1 \gamma_x(x') \frac{dx'}{x - x'}\, dx \quad \ldots \quad (4a)$$

This follows from equations (2) and (4) ; it is reasonable in both limiting cases. We shall have to assume, however, a more general relation than equation (7) for the chordwise load distribution which must include the different solutions in the limiting cases. We put

$$\gamma_x(x) = C\left(\frac{1-x}{x}\right)^n, \text{ i.e., } \Delta C_p(x) = -\frac{2}{V_0} C\left(\frac{1-x}{x}\right)^n$$

by equation (5). The constant factor C can be related to the sectional lift coefficient C_L by using equation (6). This gives

$$C_L = \frac{2}{V_0} C \int_0^1 \left(\frac{1-x}{x}\right)^n dx = \frac{2}{V_0} C \frac{\pi n}{\sin \pi n},$$

so that

$$C = \frac{V_0}{2} \frac{\sin \pi n}{\pi n} C_L .$$

Then, finally

$$\gamma_x(x) = V_0 \frac{\sin \pi n}{2\pi n} C_L \left(\frac{1-x}{x}\right)^n ; \quad \Delta C_p(x) = -\frac{\sin \pi n}{\pi n} C_L \left(\frac{1-x}{x}\right)^n \quad \ldots \quad (11)$$

which contains a single parameter, n. The value of n does not depend on x or y, but on the aspect ratio A. The function (11) fulfills the condition $\Delta C_p = 0$ at the trailing edge and the vorticity is zero there.

We can see immediately that $n \to \frac{1}{2}$ as $A \to \infty$, since equation (11) then reduces to the flat-plate distribution from equation (7). In the other extreme, $A \to 0$, the value of n must tend to one in order to obtain R. T. Jones's solution, namely $\Delta C_p = 0$ for $x > 0$; $\Delta C_p = \infty$ at $x = 0$; *i.e.*, the load is concentrated at the leading edge. Equation (11) thus represents a family of chordwise loading functions which includes both the extremes of very small and very large aspect ratio and gives a continuous variation in between. How n depends on A in the intermediate range will be determined later.

Equation (11) gives also the correct position of the aerodynamic centre in the limiting cases. This is given by

$$\frac{x_{\text{a.c.}}}{c} = \frac{1-n}{2}, \quad \ldots \quad (12)$$

(*see* Ref. 3), so that $x_{\text{a.c.}}/c = \frac{1}{4}$ for $n = \frac{1}{2}$, i.e., $A = \infty$; and $x_{\text{a.c.}} = 0$ for $n = 1$, i.e., $A = 0$.

Inserting the chordwise distribution from equation (11) into the downwash equation (4a), we obtain

$$\alpha_e = \frac{1}{2\pi}\frac{\sin \pi n}{2\pi n} C_L \int_0^1 \int_0^1 \left(\frac{1-x'}{x'}\right)^n \frac{dx'}{x-x'}\, dx$$

$$= \frac{1}{2\pi}\frac{\sin \pi n}{2\pi n} C_L \int_0^1 \left\{\frac{\pi}{\sin \pi n} - \frac{\pi}{\tan \pi n}\left(\frac{1-x}{x}\right)^n\right\} dx$$

$$= \frac{C_L}{4\pi n}(1 - \pi n \cot \pi n) \, ,$$

and finally, for the sectional lift slope,

$$a = \frac{C_L}{\alpha_e} = \frac{4\pi n}{1 - \pi n \cot \pi n} = a_0 \frac{2n}{1 - \pi n \cot \pi n} . \quad \ldots \quad (13)$$

The mean induced incidence from the chordwise and trailing vortices, α_i, can be expressed as a multiple of its value, α_{i0}, at very large aspect ratios :—

$$\alpha_i = \omega \alpha_{i0} = \frac{\omega}{2\pi}\int_{-1}^{+1} \frac{d\gamma(\eta')}{d\eta'} \frac{dn'}{\eta - \eta'} , \quad \ldots \quad (14)$$

by equation (9). The value of the ' downwash factor ' ω does not depend on x since α_i is defined as a mean value over the chord by equation (3), and we assume* that it is also independent of y. ω does depend on the aspect ratio, and we know already that $\omega = 1$ for $A = \infty$ and $\omega = 2$ for $A = 0$. Thus $\omega = 2n$ in both limiting cases, and we propose to use this relation for the whole aspect ratio range as an approximation. Physically, as the aspect ratio decreases, n represents the distortion of the chordwise loading (in the sense of concentrating the vorticity towards the leading edge) and ω represents the increase in the downwash from the streamwise vortices. These effects clearly arise from the same change in vortex pattern and so ω and n must both steadily increase with decreasing aspect ratio.

With these relations for α_e and α_i, the integral equation (10) for the spanwise loading can be generalised into :

$$\frac{2b}{ac}\gamma(\eta) = \alpha - \frac{\omega}{2\pi}\int_{-1}^{+1} \frac{d\gamma(\eta')}{d\eta'} \frac{d\eta'}{\eta - \eta'} , \quad \ldots \quad (15)$$

which is of the same type as Prandtl's original equation and can be solved in the same way. For practical purposes it appears best to employ Multhopp's method[17], where equation (15) is transformed into a system of linear equations :

$$\gamma_\nu\left(b_{\nu\nu} + \frac{2b}{\omega a c_\nu}\right) = \frac{\alpha_\nu}{\omega} + \sum_{n=1}^{m}{}' b_{\nu n}\gamma_n . \quad \ldots \quad (16)$$

---

* The assumption that both n and ω do not depend on y may lead to errors near the wing tips. It implies that the chordwise load distribution is of the same type at all spanwise stations and a forward shift of the aerodynamic centre as the tips are approached is not represented. The error cannot be serious, however, as the lift falls to zero there (*see* also section 2.6). A refinement of the present theory in this direction is, of course, possible. On the other hand, the wing tips are much affected by the presence of the tip vortex (*see* sections 2.6 and 3.8), and the interest in the precise chordwise loading, as given by linearised theory, is therefore much reduced.

The suffix ν indicates that the respective quantity is taken at a fixed spanwise position ν. The $b_{\nu\nu}$ and $b_{\nu n}$ are known coefficients and can be found in Refs. 3 and 17. From this the spanwise loading can be determined in about the same time as the ordinary large aspect ratio calculation of Multhopp[17] (about one computer-hour), and the chordwise loading found from equation (11). The overall lift coefficient is

$$\bar{C}_L = A \int_{-1}^{+1} \gamma(\eta)\, d\eta \; . \qquad (17)$$

It remains to determine the shape parameter n on which both sectional lift slope a and downwash factor ω depend. For this purpose, we consider again the limiting case of very small aspect ratio. As $A \rightarrow 0$, the plan-form term

$$\frac{2b}{ac} = \frac{2}{ac/\bar{c}} A$$

in equation (15) tends to zero, provided A goes to zero more quickly than a. If the above term can be ignored as compared with α, equation (15) reduces to

$$\alpha = \frac{\omega}{2\pi} \int_{-1}^{+1} \frac{d\gamma}{d\eta'} \frac{d\eta'}{\eta - \eta'} = \frac{1}{\pi} \int_{-1}^{+1} \frac{d\gamma}{d\eta'} \frac{d\eta'}{\eta - \eta'} = \alpha_i \qquad (18)$$

since $\omega \rightarrow 2$ at the same time. The solution of this equation is

$$\gamma(\eta) = \alpha\sqrt{(1 - \eta^2)} \; , \qquad (19)$$

i.e., the span loading becomes elliptic, and the overall lift is, by equation (17),

$$\frac{\bar{C}_L}{\alpha} = A \int_{-1}^{+1} \sqrt{(1 - \eta^2)}\, d\eta = \frac{\pi}{2} A \rightarrow 0 \text{ as } A \rightarrow 0 \; . \qquad (20)$$

These results agree with those of R. T. Jones.

From equations (18) and (19),

$$\alpha_i = \omega \frac{\bar{C}_L}{\pi A} = \omega \frac{\alpha}{2} \rightarrow \alpha \text{ as } \omega \rightarrow 2, \; i.e., \text{ as } A \rightarrow 0 \; .$$

This means that the chordwise and trailing vortices alone fulfil the boundary condition, the downwash being produced in equal parts by the chordwise and trailing vortices since

$$\alpha_{i0} = \frac{1}{\pi A} \bar{C}_L = \frac{1}{\pi A} \cdot \frac{\pi}{2} A\alpha = \frac{\alpha}{2}$$

for $A = 0$, by equations (9), (19) and (20). Also, for wings of elliptic plan form, $C_L = \bar{C}_L$, by equation (19), so that $\alpha_e = \bar{C}_L/a$. Hence, from the boundary condition $\alpha = \alpha_e + \alpha_i$:

$$\frac{\bar{C}_L}{\alpha} = \frac{1}{\dfrac{1}{a} + \dfrac{\omega}{\pi A}} = \frac{4\pi n}{1 - \pi n \cot \pi n + \dfrac{8n^2}{A}} \; , \qquad (21)$$

from equation (13) and $\omega = 2n$. Combining equations (20) and (21), we find that n behaves like

$$n = 1 - \sqrt{\frac{A}{8}} \rightarrow 1 \text{ as } A \rightarrow 0 \qquad (22)$$

for small aspect ratios. This gives for the sectional lift slope

$$a = 2\pi\sqrt{\frac{A}{2}} \rightarrow 0 \text{ as } A \rightarrow 0, \quad \ldots \quad (23)$$

and for the effective incidence

$$\frac{\alpha_e}{\alpha} = \sqrt{\frac{A}{8}} \rightarrow 0 \text{ as } A \rightarrow 0, \quad \ldots \quad (24)$$

by equation (20), in agreement with R. T. Jones's theory. Equation (23) is consistent with the initial assumption that $A/a \rightarrow 0$ as $A \rightarrow 0$.

Equation (22) can be used to derive a general relation between n and A for the whole aspect ratio range. At the high aspect ratio end, n must approach the value $\frac{1}{2}$ and it is known from experience that n does not appreciably differ from $\frac{1}{2}$ for aspect ratios of about 6 and greater. A simple monotonic function $n(A)$ to fulfil the condition (22), and which also approaches the value $n = \frac{1}{2}$ for very large aspect ratio in a reasonable manner, is

$$n = 1 - \frac{1}{2\left\{1 + \left(\frac{2}{A}\right)^2\right\}^{1/4}} \quad \ldots \quad (25a)$$

or, more generally,

$$n = 1 - \frac{1}{2\left\{1 + \left(\frac{a_0}{\pi A}\right)^2\right\}^{1/4}}. \quad \ldots \quad (25b)$$

This approximation is quite sufficient for practical purposes. At any rate, existing theories cannot provide a more accurate relation. Thus, with n being known, the load over the surface of any given wing can be determined.

There are various experimental means of checking the accuracy of the present method. The value of n from equation (25) can be checked directly against measured values of the position of the centre of pressure, using equation (12). It is found that the experimental values from Ref. 15 and the theoretical values are identical within the accuracy of the experiment. The values of a from equation (13) can be compared with the slopes of the $C_T(C_N{}^2)$ curves, as plotted in Fig. 5, and again good agreement is found. Finally, overall lift coefficients for a series of rectangular wings have been calculated* from equation (16) and compared with measured values from various tests. Fig. 6 shows that the measured lift is well predicted throughout the whole aspect ratio range.

2.3. *Comparison with the Results of Other Calculations.*—Some indication of the accuracy of the new method can be given by comparing the results with those obtained in some special cases by the most thorough mathematical treatment so far. These are: the wing of circular plan form by Kinner[16]; some elliptic wings by Krienes[25]; and some rectangular wings by Wieghardt[26]. In the latter case the spanwise loading was assumed to be elliptic so that the results are likely to be slightly wrong for aspect ratios above one.

By considering the results obtained for the chordwise loading, we find that equation (11) is a good approximation in all cases. In particular, the position of the aerodynamic centre, found by various methods and plotted in Fig. 8, is well approximated by equation (25); this agrees rather better with Wieghardt's results in the lower aspect ratio range than with the other less accurate calculations, as one would expect.

* In this calculation allowance has been made for the thickness/chord ratio of the wing by putting $\varepsilon = 0{\cdot}08$; and for the effect of the boundary layer by putting $k = 0{\cdot}92$. Hence $a_0 = 0{\cdot}92 \times 1{\cdot}08 \times 2\pi = 2\pi$.

Fig. 9 shows a typical example of the chordwise loadings obtained by the various methods, illustrating the degrees of approximation. The other methods are based in one way or another on the series of functions devised by Birnbaum[12] of which the first term is the flat-plate distribution from equation (4). The number of terms taken determines at how many points along the chord the boundary condition can be fulfilled. Both the number and position chosen for these points affect the result. Obviously, two terms (Falkner[23], Multhopp)[27] can only give a crude approximation. The three-term approximation of Scholz[19] lies to the other side of the present one, whereas Wieghardt's four-term approximation[26] reverts to the original side*. Considering the general tendency of the various approximations, it appears that equation (11) with the appropriate value of n from equation (25) gives a very satisfactory approximation.

It may seem surprising that a single term should give at least as good an approximation as four terms of the ordinary series. This may be due to the fact that the original flat-plate distribution is very unsuitable to start with and that the further terms do not represent well enough the necessary modifications to the loading. The second term in Birnbaum's series is derived from the flow around a two-dimensional circular-arc cambered aerofoil which is quite different from the flow and the vortex system of a small aspect ratio wing. It may be said now, that Birnbaum's functions could really not have been expected to be useful unless a number of terms were taken (at least four terms, as may be seen in the present case).

It should be possible to find the value of the sectional lift slope a from the theories mentioned above as $a = -C_N^2/C_T$. Unfortunately, only Kinner has considered the suction force at the leading edge and thus C_T in some detail. He finds that a has a constant value, independent of the incidence, as in any linearised theory; but he is not able to give a direct derivation of the value of C_T so that values of a cannot be obtained for the present purpose†.

Calculated overall lift values from the present method are compared with those of Krienes for elliptic wings in Fig. 7. Complete agreement is found. Also, the span loading is found to be nearly elliptic by both methods. Overall lift values of rectangular wings are considered in Fig. 6. The results from the present method agree with Wieghardt's results in the low aspect ratio range up to one. Other calculation methods give different answers from the present method mainly in the higher aspect ratio range, but experimental evidence favours the latter.

The case of the circular plate, which has also been treated by Multhopp[27], may be briefly considered. Multhopp has shown that the four chordwise terms taken by Kinner are not sufficient to give a correct value of the overall lift. With five terms, $\bar{C}_L/\alpha = 1 \cdot 804$, whereas Kinner gave $1 \cdot 82$. Multhopp found $1 \cdot 799$, and the present method gives $1 \cdot 805$. The position of the overall aerodynamic centre, measured from the leading edge at the centre in terms of the centre line chord, is $0 \cdot 243$ from Kinner (four terms); $0 \cdot 236$ from Multhopp; and $0 \cdot 231$ from the present method. The span loading distribution from the present method agrees with that of Kinner.

On the whole, the agreement with the results of Kinner, Krienes, and Wieghardt is such that the present method can also be regarded as an interpolation between these results for special cases, which are the most accurate so far available.

2.4. *The Three-quarter Chord Theorem.*—In various methods use has been made of the so-called 'three-quarter chord theorem' to refine Prandtl's aerofoil theory. It is in these methods only that the concept of a lifting line must necessarily be introduced. The three-quarter chord theorem was derived by Pistolesi[28] for the properties of the bound vortices on a wing of infinite aspect ratio. It states that, concentrating the lift at the quarter-chord line, the downwash produced by it at the three-quarter chord line is the same as that produced by the flat-plate vortex distribution, equation (7), which is constant along the chord. It has subsequently been applied to the combined effect of bound and trailing vortices on wings of finite aspect ratio in that the

* It should also be borne in mind that Wieghardt's assumption of elliptic span loading leads to rather high C_L values at the centre, *see* Fig. 10.

† It is found, however, that a is considerably smaller than $a_0 = 2\pi$ for the circular plate ($A = 1 \cdot 27$).

strength of an isolated vortex line at quarter-chord is so determined as to give a downwash at three-quarters chord from the leading edge on the centre-line of the wing which is equal to the given geometric incidence. This is not correct, but we shall see that it is possible in some cases that the various errors involved just cancel each other.

Assuming elliptic span loading,

$$\Gamma = \Gamma_0\sqrt{(1-\eta^2)} = \frac{2V_0\bar{c}}{\pi}\,\bar{C}_L\,\sqrt{(1-\eta^2)}, \qquad (25)$$

we find that the downwash from a straight lifting line at quarter-chord and the corresponding trailing vortices induced at the three-quarter chord point on the centre-line is given by (*see* Ref. 26)

$$\frac{v_z}{V_0} = \frac{2}{\pi^2 A}\,\bar{C}_L\left\{\frac{\pi}{2} + \frac{\sqrt{\{(4/\pi A)^2+1\}}}{4/\pi A}\,\mathbf{E}(k^2)\right\},$$

where $\mathbf{E}$ is the complete elliptic integral with the modulus

$$k^2 = \frac{1}{1+(4/\pi A)^2}. \qquad (26)$$

Equating v_z/V_0 to the geometric incidence α, we obtain

$$\frac{\bar{C}_L}{\alpha} = \frac{2\pi}{\sqrt{\{1+(4/\pi A)^2\}}\mathbf{E}(k^2) + 2/A}. \qquad (27)$$

This can be simplified by using the approximation

$$\mathbf{E}(k^2) \simeq \sqrt{\left\{\frac{\pi^2}{4}(1-k^2) + k^2\right\}}, \qquad (28)$$

which leads to

$$\frac{\bar{C}_L}{\alpha} = \frac{2\pi}{\sqrt{\{1+(2/A)^2\}} + 2/A} = \frac{a_0}{\sqrt{\{1+(a_0/\pi A)^2\}} + a_0/\pi A}. \qquad (29)$$

This relation was first derived by H. B. Helmbold[29] and again by H. Multhopp (*see* Ref. 30), and has frequently been used or derived again by several authors, as recently by N. Scholz[19] and F. W. Diederich[31].

Equation (29) can be written in terms of a sectional lift slope, a, and a downwash factor, ω. Determining that part of the downwash which is due to the lifting line, we find

$$\frac{v_{z1}}{V_0} = \alpha_e = \frac{2\bar{C}_L}{\pi A}\left[\sqrt{\left\{1+(\tfrac{1}{4}\pi A)^2\right\}}\mathbf{E}(k^2) - \frac{\mathbf{K}(k^2)}{\sqrt{\{1+(\frac{1}{4}\pi A)^2\}}}\right],$$

where $\mathbf{K}$ is the elliptic integral of the first kind, with k from equation (26). Hence,

$$a = \frac{C_L}{\alpha_e} = \frac{\bar{C}_L}{\alpha_e} = \frac{\pi^2 A}{2}\,\frac{1}{\left[\sqrt{\{1+(\frac{1}{4}\pi A)^2\}}\mathbf{E}(k^2) - \frac{\mathbf{K}(k^2)}{\sqrt{\{1+(\frac{1}{4}\pi A)^2\}}}\right]}. \qquad (30)$$

Combining equations (21) and (29) and inserting a from equation (30), we obtain for the downwash factor

$$\omega = 1 + \sqrt{\left\{1+\left(\frac{A}{2}\right)^2\right\}} - \frac{\pi A}{a}. \qquad (31)$$

From equation (30) the value of a tends to infinity as the aspect ratio tends to zero, Fig. 11, whereas it should tend to zero. This is compensated for (so far as overall loads are concerned) by the values of ω from equation (31) being much greater than those of the present theory; unlike a, ω does, however, tend to the correct limit (2) for zero aspect ratio.

Further, the values of a and ω implied by the three-quarter chord theorem are more sensitive to the shape of the spanwise loading than could be expected from physical considerations; this may be seen from Figs. 11 and 12 where curves are given for a constant loading as well as an elliptical one. The contribution of a bound vortex line of constant strength $\Gamma = \Gamma_0 = \frac{1}{2} V_0 \bar{c} \bar{C}_L$ along the span is obtained from

$$\alpha_e = \frac{\bar{C}_L}{2\pi} \frac{1}{\sqrt{(1 + 1/A^2)}}, \qquad (32)$$

which gives

$$a = 2\pi \sqrt{(1 + 1/A^2)}. \qquad (33)$$

Thus the three-quarter chord theorem has basically unsound physical implications and the fact that it provides reasonable answers in some applications must be largely fortuitous.

The value of a from equation (13) can be obtained from a lifting line of either constant or elliptic spanwise strength if the chordwise position of the point at which the downwash is calculated (' incidence point ') is varied with aspect ratio. The result is plotted in Fig. 13 and it can be seen that it is correct to take the three-quarter chord point only for a wing of infinite aspect ratio, in accordance with Pistolesi's original derivation. With decreasing aspect ratio the position of the incidence point should move forward and reach the leading edge at $A = 0$, in accordance with R. T. Jones's results.

In view of this, it is remarkable how well Helmbold's formula (29) agrees with the results of Krienes and those of the present method, as shown in Fig. 7. This is due to the two errors in a and ω opposing each other, and the error involved in the approximation from equation (28) also has a beneficial effect. Thus, in spite of the fortuity of the agreement, Helmbold's formula may be used for some special purposes (*see*, *e.g.*, sections 2.6 and 4 of this report) and also to obtain a quick estimate.

It becomes very doubtful, however, whether the three-quarter chord theorem can profitably be applied to obtain more detailed span loading distributions by calculating the downwash from a lifting line at the three-quarter chord points of several spanwise stations, thus upsetting the equilibrium of errors. The results of Weissinger's L-method[21], and those of Young[22] which are based on this, may therefore be appreciably wrong, as is demonstrated by the examples given in Fig. 6.

2.5. *Induced Drag*.—In experiencing a drag force, the wing which moves at a velocity V_0 performs the work $D_i V_0$ per unit time on the flow. This makes itself felt as an increase of the kinetic energy of the flow in that a certain mass of air $\rho V_0 S'$ is moving downward at a uniform velocity $v_{z\infty}$ far behind the wing, where $v_{z\infty}$ is the downwash at the vortex sheet. The kinetic energy given to the flow per unit time is then $\rho V_0 S' v_{z\infty}^2/2$. Hence,

$$D_i V_0 = \rho V_0 S' \frac{v_{z\infty}^2}{2}.$$

On the other hand, the momentum of the air moving downwards is equal to the lift force on the wing, *i.e.*,

$$L = \rho V_0 S' v_{z\infty}.$$

This gives a relation between the overall lift and the overall induced drag forces :—

$$D_i = \frac{1}{2} \frac{v_{z\infty}}{V_0} L \text{ or } \bar{C}_{Di} = \frac{1}{2} \frac{v_{z\infty}}{V_0} \bar{C}_L. \qquad (34)$$

The derivation of this formula, which follows that in Ref. 32, applies to any wing, whether its aspect ratio is large or small, if $v_{z\infty}$ is taken as the mean downwash at the vortex sheet far behind the wing.

The induced drag at a given overall lift is at its minimum if the downwash $v_{z\infty}$ is constant along the span. In that case, consideration of the flow in the Trefftz-plane leads to elliptic span loading and gives

$$\frac{v_{z\infty}}{V_0} = \frac{2\bar{C}_L}{\pi A} = 2\alpha_{i0} \qquad (35)$$

so that, by equation (34),

$$\bar{C}_{Di} = \frac{\bar{C}_L{}^2}{\pi A} = \alpha_{i0}\bar{C}_L . \qquad (36)$$

This is the well-known relation of M. M. Munk[33] which was originally derived for wings of very large aspect ratio and then shown to hold also for wings of very small aspect ratio by N. F. Ward[34]. Clearly, it holds also for wings of any aspect ratio.

Equation (36) may seem to contradict our concept of the mean downwash at the wing being $a_i = \omega\alpha_{i0}$, as the induced drag is commonly assumed to be equal to $\alpha_i\bar{C}_L$, which would give $\bar{C}_{Di} = \omega\bar{C}_L{}^2/\pi A$. However, in determining the induced drag correctly from the Kutta-Joukowski theorem, the product of the local downwash and the local vortex strength must be integrated along the chord of the wing, and this is not necessarily equal to the product of the mean downwash and the mean lift along chord. In the extreme case of a wing of very small aspect ratio as sketched in Fig. 4, where the lift is nearly all concentrated near the leading edge, the downwash from the trailing and chordwise vortices at the position of the spanwise vortex is obviously equal to $a_{i0}V_0$, which leads to equation (36), whereas the mean downwash across the whole chord is very nearly $\omega\alpha_{i0} \simeq 2\alpha_{i0}$, which confirms equation (14).

Equation (36) can be generalised for arbitrary wing plan forms, which do not give minimum induced drag. In that case,

$$\bar{C}_{Di} = A\int_{-1}^{+1} \gamma\,(\eta)\;\alpha_{i0}\,(\eta)\;d\eta \qquad (37)$$

where α_{i0} is given by equation (9) for a known span loading $\gamma(\eta)$, which can be found from equation (16). This relation was checked against measured values from the series of rectangular wings from Ref. 15. Good agreement was found throughout the whole aspect ratio range.

2.6. *Non-linear Effects.*—The theory developed so far always leads to linear relations between lift and incidence. It has been observed, however, that the lift of small aspect ratio wings is by no means a linear function of the angle of incidence but rises more steeply. Various hypotheses have been put forward to explain this effect (*see, e.g.*, Refs. 35, 36 and 37). Here, we interpret the physical phenomena as follows :

Consider the flow past a flat plate of, say, rectangular plan-form, as in Fig. 14. If this plate is inclined against the stream at a large angle near 90 deg, the flow will separate at all four edges, forming a dead-air region behind the plate, like Kirchhoff's flow ; the dead-air being separated from the main stream by a surface of discontinuity which may be interpreted as a vortex sheet, *see* Fig. 14a. At moderate incidences, below α_{max} (which normally gives maximum lift), the flow is able to take the turn around the leading edge of the wing without separating, especially if the leading edge is suitably rounded off. In this stage, the flow separates from only three edges of the wing, Fig. 14b, forming a vortex sheet which consists of a horizontal part, originating from the trailing edge, and two vertical sheets attached to it, originating from the two sides of the plate. With the flow having broken into the dead-air region, the latter disappears. At still smaller incidences, below a certain value α_s, the flow may also attach to the sides of the wing, especially if these are rounded off, Fig. 14c, and only the vortex sheet from the trailing edge remains. This is the case that has been considered so far, leading to linear relations; any deviations from it must be connected with the existence of the vertical vortex sheets at the sides.

This problem has been treated by W. Mangler[38] by making use of the fact that a spanwise cross-section through the vortex sheet has the same shape as that obtained behind a wing with solid end-plates attached to it. If the height of the 'end-plate vortex,' or 'tip vortex' is known, the lift change due to its presence can be found as described in Refs. 39, 40 and 41 for the case of minimum induced drag. The overall lift from linear theory can then be approximated by Helmbold's equation (29), and the effect of the end-plates can be expressed as a factor, $1/\varkappa$, to the aspect ratio. Hence the overall lift is given by

$$\frac{\bar{C}_L}{\alpha} = \frac{a_0}{\sqrt{\left\{1 + \left(\varkappa \frac{a_0}{\pi A}\right)^2\right\}} + \varkappa \frac{a_0}{\pi A}}, \qquad \ldots \quad (38)$$

or, at the same incidence,

$$\frac{\bar{C}_L}{\bar{C}_{L\,0}} = \frac{\sqrt{\left\{1 + \left(\frac{a_0}{\pi A}\right)^2\right\}} + \frac{a_0}{\pi A}}{\sqrt{\left\{1 + \left(\varkappa \frac{a_0}{\pi A}\right)^2\right\}} + \varkappa \frac{a_0}{\pi A}}, \qquad \ldots \quad (39)$$

where $\bar{C}_{L\,0}$ is the overall lift coefficient as obtained from linear theory. The proper values of $\bar{C}_{L\,0}$ for the given wing from equation (17) may be taken here instead of the approximate value from equation (29). The value of $\varkappa$ depends only on the ratio, h/b, between end-plate height and wing span, and can be taken from Refs. 39 and 40, *see* also Ref. 41. $\varkappa = 1$ for $h/b = 0$; $\varkappa < 1$ for $h/b \neq 0$.

The calculation method of Ref. 39 does not give the spanwise loadings of a given wing both with and without end-plates but only those of a wing without end-plates that has elliptic span loading and of another wing with end-plates, each giving minimum induced drag. It is assumed here that the difference, ΔC_L, in span loading between the two minimum induced drag Wings can be taken as the difference in spanwise loading due to end-plates (or due to the tip vortex) for a given wing whose basic loading is not elliptic. In this case,

$$\Delta C_L(\eta)\,\frac{c(\eta)}{\bar{c}} = C_{L\,0}\left\{\frac{\sqrt{\left\{1 + \left(\frac{a_0}{\pi A}\right)^2\right\}} + \frac{a_0}{\pi A}}{\sqrt{\left\{1 + \left(\varkappa \frac{a_0}{\pi A}\right)^2\right\}} + \varkappa \frac{a_0}{\pi A}}\; l\left(\eta\,;\frac{h}{b}\right) - l\,(\eta\,;0)\right\} \qquad \ldots \quad (40)$$

where l ls a known function of the spanwise co-ordinate and of the ratio between end-plate height and wing span. Curves of $l(\eta\,;h/b)$ are plotted in Ref. 41.

The difficulty lies in determining the value of h/b, which will depend on the incidence of the wing and also on the tip shape. Since the shape of the tip vortex is hardly investigated at all, we can only make plausible suggestions. According to W. Mangler[38],

$$\frac{h}{b} = \frac{\alpha}{2}\frac{c_T}{b} = \frac{\alpha}{2}\frac{c_T}{\bar{c}}\cdot\frac{1}{A}, \qquad \ldots \quad (41)$$

where c_T is the tip chord. This implies that the height of the tip vortex increases gradually with incidence, and the lift increment will increase correspondingly, being zero at $\alpha = 0$. Hence, the initial lift slope $\bar{C}_L/\alpha$ at zero lift is the same as that given by linearised theory.

Equation (41) will be sufficiently accurate for many practical purposes, at least for the determination of the overall lift*, as shown in Fig. 15.

It will be seen that the lift increment due to the tip vortex is only approximately a quadratic function of the incidence. As an illustration, the spanwise loadings of a square wing are shown in Fig. 16.

It can be seen from equation (41) and Fig. 15 that the non-linear lift increase becomes smaller with increasing aspect ratio, although the height of the tip vortex does not change. This explains why the effect of the tip vortex has rarely been noticed for wings of moderate and large aspect ratio although it always existed.

It may be noted that the points in Fig. 15 from Scholz[19] for wings of aspect ratios 0·7 ; 1·2 ; and 2·2 agree with those from other experiments for aspect ratios 0·5 ; 1·0 ; and 2·0. Whereas the latter wings had square cut tips, those of Scholz had rounded tip fairings added to wings whose basic aspect ratios were 0·5 ; 1·0 ; and 2·0 again. The agreement shows that the span of the trailing edge determines the shape of the wake and is, therefore, the decisive parameter in determining the effective aspect ratio, and not the maximum span from tip to tip.

It is difficult to assess the effect of the tip vortex on the drag. Primarily, the induced drag is reduced due to the aspect ratio being effectively increased. On the other hand, however, the extra lift from the tip vortex will have a chordwise distribution different from that of the linearised theory, being concentrated further back on the chord where the height of the vortex sheet is greatest. (*see, e.g.*, Ref. 42.) This results in an additional form drag which counteracts the initial reduction of the induced drag. It may well be that all the extra lift $\Delta \bar{C}_L$ from the tip vortex acts further back on the aerofoil and does not produce a suction force at the leading edge (for a flat plate). In that case,

$$\bar{C}_D = \bar{C}_{D0} + \frac{\bar{C}_{L0}^{\,2}}{\pi A} + \Delta \bar{C}_L \alpha \,.$$

This appears to be confirmed by experiments.

The rearward position of the non-linear lift increment has an appreciable effect on the position of the aerodynamic centre. This is demonstrated for the case of a square wing in Fig. 17. Two more approximations for the height of the end-plate vortex are suggested here :

$$\frac{h}{b} = \frac{\alpha - \alpha_s}{2} \frac{c_T}{\bar{c}} \cdot \frac{1}{A} , \qquad \ldots \qquad (42)$$

which differs from equation (41) in that the tip vortex is assumed to exist only when the incidence is greater than a 'separation incidence,' α_s, which is 4 deg in the present case † ; and

$$\frac{h}{b} = \alpha \frac{\alpha - \alpha_s}{\alpha_m - \alpha_s} \frac{c_T}{\bar{c}} \frac{1}{A} , \qquad \ldots \qquad (43)$$

where it is assumed that the flow separates first near the trailing edge at $\alpha = \alpha_s$ and then extends gradually over the tip chord until the leading edge is reached at $\alpha = \alpha_m$. (*see* Ref. 41.) The three different estimates do not lead to very different values for the overall lift, but the position of the aerodynamic centre obtained varies considerably. Further, it is essential to know where the resultant of the non-linear lift increment acts, and it may not be accurate enough to assume it to act at the three-quarter chord line. Further work on the flow in the tip region in the presence of the tip vortex is therefore needed. There is, however, no doubt that the tip vortex is responsible for the non-linear effects.

---

* That good agreement with experiments could not be obtained from the method in Ref. 38 is due to the fact that the linear part of the lift was then calculated from Prandtl's original formula for very large aspect ratio.

† This delay in the first appearance of the tip vortex is also apparent in the experiments of Scholz in Fig. 15, evidently being caused by the well-rounded tip fairing.

3. *Swept Wings.*—It is difficult to give a precise definition of a swept wing as opposed to a straight wing. For instance, a highly tapered wing of very small aspect ratio with its leading edge swept back by the same amount as its trailing edge is swept forward might, on the whole, be considered as an unswept wing although localised sweep effects near the leading and trailing edges will no doubt occur. In most cases of practical interest such extremes will, however, not occur and we shall consider a wing as being swept if its mid-chord line is not straight but has a kink at the line of symmetry of the wing.

3.1. *Description of the General Approach.*—The general approach used in extending the calculation method to swept wings is the same as above and can be described under three main headings :

(i) The lifting surface and its wake are replaced by a system of vortices, and the vorticity vector at any point is again subdivided into a component along the span (' spanwise vortex ') and into a component along the main stream (' chordwise vortex ' on the lifting surface ; ' trailing vortex' in the wake). The spanwise vortices are no longer normal to the direction of the free stream, Fig. 18. They still produce the lift force on the aerofoil and no overall drag force ; the trailing vortices are responsible for the drag of the aerofoil in inviscid flow ; chordwise and trailing vortices do not produce a lift force. The downwash at any spanwise station is again subdivided into the ' effective incidence,' α_e, from the spanwise vortices, equation (2) ; and the ' induced incidence,' α_i, from the streamwise vortices, equation (3). The boundary condition is then $\alpha = \alpha_e + \alpha_i$, as before, which is thus fulfilled at any spanwise station only for mean values over the chord of the downwash $v_z = v_{z1}(x) + v_{z2}(x)$. All angles are assumed to be small.

(ii) The effective incidence is determined from the hypothesis that the mean downwash over the chord,

$$\alpha_e = \frac{1}{V_0}\int_0^1 v_{z1}(x)\, dx \, ,$$

equation (2), which is induced by the spanwise vortices at any spanwise station, is, to a first approximation, the same as the mean value of the downwash v_{z0} which is induced by vortices having the same direction and pattern and the same chordwise distribution as those at the station but of infinite length on either side of it. Thus

$$\alpha_e = \frac{1}{V_0}\int_0^1 \frac{v_{z0}(x)}{V_0}\, dx \, , \qquad \text{(44)}$$

which corresponds to equation (2). The suffix 0 in v_{z0} is used here to signify that the quantity is determined for a wing of infinite aspect ratio.

(iii) The induced incidence α_i at any spanwise station is taken as a multiple of the downwash, α_{i0}, far behind the wing at that station. This is expressed by equation (14), where the ' downwash factor ' ω varies between 1 (for very large aspect ratios) and 2 (for very small aspect ratios).

The method is thus basically the same for both straight and swept wings. The only new problem arises from the fact that the spanwise vortices change their direction at the centre of swept wings, even on a wing of infinite aspect ratio. Thus the determination of v_{z0} at the centre is also affected. Whereas v_{z0} is found from a two-dimensional vortex distribution for straight wings and for the sheared part of swept wings from equation (4), the centre of swept wings requires the treatment of a special vortex distribution with a kink. At the centre, v_{z0} is not the same as v_{z1} from equation (4) which holds only for two-dimensional wings without kinks in the vortex lines. We therefore need a new downwash equation to determine v_{z0} at the centre of a swept wing of infinite aspect ratio, to replace equation (4). This problem has first been treated in Ref. 44 and again in Ref. 3, and it will be further discussed in section 3.2 below because of its fundamental importance.

In linearised theory, the effective incidence $\alpha_e(\eta)$ at any spanwise station η is still proportional to the local lift coefficient $C_L(\eta)$ at that station so that $C_L(\eta) = a(\eta)\alpha_e(\eta)$, where $a(\eta)$ is the 'sectional lift slope' at that station. The boundary condition, $\alpha_e = \alpha - \alpha_i$, can then be written in the form of equation (15), *i.e.*, the loading equation is of the same type as Prandtl's original equation for both straight and swept wings of any aspect ratio.

Values for the sectional lift slope, a and for the downwash factor ω, must now be found. Both will depend not only on the aspect ratio, as for straight wings, but also on the angle of sweep, φ ; a also depends on the spanwise co-ordinate η. It is convenient to relate both these parameters to the chordwise vortex distribution $\gamma_x(x)$ which in turn is related to the chordwise load distribution $\Delta C_p(x)$. $\Delta C_p(x)$ from equation (11) is still a suitable function because it is valid in both the limiting cases.

It will be seen that both a and ω depend on the value of the parameter n in equation (11). a can be related to n if the downwash equation for the spanwise vortices is known (*see* section 3.2). $\omega \fallingdotseq 2n$ in the limiting cases, and this relation is assumed to hold everywhere. The main physical condition that the downwash from the chordwise and trailing vortices increases as the chordwise loading moves forward, and *vice versa*, is thus fulfilled automatically. The problem now reduces to that of finding the value of n, which will depend on the aspect ratio of the wing, on the angle of sweep, and on the spanwise co-ordinate. With n known, values for a and ω can be found and subsequently the spanwise load distribution from equation (16) and the chordwise load distribution from equation (11).

3.2. *The Downwash on the Centre-line.*—As explained above, the determination of the downwash induced by the spanwise vortices and the subsequent solution of this downwash equation are the only new problems of importance that occur on swept wings. Although the downwash equation and its solution have previously been derived in Refs. 44 and 3, some further discussion may be justified in order to explain the nature of the approximations made, so that it can be more readily compared with other methods (Ref. 45).

3.2.1. *The vortex system.*—The characteristics of the vortex system in the central region of a swept wing can be seen by considering the simple case of a wing of constant chord and infinite aspect ratio as shown in Fig. 18. For a flat wing at incidence, the vorticity vector will be parallel to the leading edge at any point on the wing chord if the distance from the centre-line is large. There is thus no chordwise vortex component on this 'sheared part' of the wing. When the centre is approached, the vorticity vector curves round and is assumed to cross the centre-line at right-angles. Since the local lift coefficient at the centre is not necessarily the same as that on the sheared part of the wing, some of the vortex lines may leave the wing surface and continue as trailing vortices in the wake. The curvature of the vortex lines on the wing surface means the formation of chordwise vortices. These increase in strength as the centre is approached; they change sign discontinuously at any point on the centre-line except at the trailing edge (*see* Fig. 18), unlike the trailing vortices which also change sign but go continuously through zero at $y = 0$. This discontinuity causes the velocity v_z induced by the chordwise vortices to tend logarithmically to infinity* as $y \rightarrow 0$. The spanwise vortices, on the other hand, change their direction discontinuously by the angle 2φ. This produces another logarithmically infinite velocity† at $y = 0$, as has been shown in Ref. 3, which cancels exactly the infinity from the chordwise vortices. This is, of course, only another way of stating that the actual, curved, vortex lines are continuous. For the present purpose, we shall have to consider the kinked spanwise vortices alone.

* It may be remembered that two isolated vortex lines of infinite length, parallel to each other and of opposite direction, cancel each other if their respective strengths remain constant when they approach each other; but produce a doublet if their strength increases with the inverse of their distance. In the present case, however, such vortex lines are distributed over a surface, and an infinite velocity is produced even though the vortex strength at the discontinuity remains finite.

† It may be noted that the same infinity occurs when the kinked vortex lines are considered as the limits of hyperbolae, in which case the direction of the vorticity vector would not change discontinuously at the centre-line but would be defined as normal to the centre-line.

Mathematically, these considerations can be of some consequence. In an ordinary lifting-surface theory, the determination of the downwash leads to a double integral over the wing surface and the wake, containing the unknown vortex distribution in the integrand. This integral is usually reduced, by an integration, to a single integral with respect to one of the co-ordinates to make an approximate solution possible. Such an integration in steps is permissible where a curvilinear system of co-ordinates is used with one variable measured along the actual vortex lines (the shape of which is, however, unknown). An integration in steps using, for instance, the co-ordinates x and $y/\cos\varphi$ is not permissible because of the discontinuity of the vortex components in these directions.

3.2.2. *The downwash on the surface of a thick aerofoil with uniform load along the span.*—A chordwise distribution $\gamma_x(x)$ of straight vortex lines of infinite length in the plane $z = 0$, kinked at $y = 0$ and swept by an angle of φ, produces a logarithmically infinite downwash at $0 \leqslant x \leqslant 1$; $y = 0$; $z = 0$, as shown in Refs. 3 and 44. This implies that the 'wing surface,' obtained by integrating v_z/V_0, is not in the plane $z = 0$ but is cambered and twisted, with a vertical tangent at $y = 0$. Such a wing cannot be treated by linearised theory where the vortex distribution is placed in the plane $z = 0$, and the above result has therefore no physical meaning. The problem could be treated by successive approximations, *i.e.*, by putting the vortex distribution on the curved surface thus obtained, recalculating the downwash, and so forth. This is necessarily a cumbersome process, and convergence is not assured if the distribution at $z = 0$ is taken as the first approximation.

It is much simpler to calculate the downwash which is induced on the surface of a wing of non-zero thickness by a vortex distribution situated in the plane $z = 0$. This is, after all, the case of practical interest, and singularities cannot occur if the vortex distribution is inside the aerofoil contour. This has been done in Refs. 3 and 44, and it was found that the downwash at the centre section could be approximated by

$$\frac{v_{z0}}{V_0} = \frac{1}{2\pi V_0}\left\{\int_0^1 \gamma_x(x')\,\frac{dx'}{x - x'} + \pi \tan\varphi\,\gamma_x(x)\right\}. \quad (45)$$

According to our hypothesis, this relation can also be applied to wings with non-uniform spanwise loading. For a flat wing, such that $v_{z0} = \text{const} = \alpha_{e0} V_0$, equation (45) has the solution

$$\gamma_x(x) = 2\alpha_{e0}\, V_0 \cos\varphi \left(\frac{1 - x}{x}\right)^{n_0}, \quad (46)$$

where

$$n_0 = \tfrac{1}{2}\left(1 - \frac{\varphi}{\pi/2}\right). \quad (47)$$

Equation (45) was also used for γ_x-distributions which differ from that and which are associated with cambered wings, *see* Ref. 4.

Equation (45) cannot easily be verified analytically, and numerical examples have been given in Refs. 3 and 44 for several vortex distribution and aerofoil shapes of different thickness/chord ratios to justify it. Since equation (45) forms the basis for the present work on swept wings, some further numerical examples may be given here.

Assuming a certain distribution $\gamma_x(x)$, the downwash induced by it at $y = 0$ was first calculated from the Biot-Savart law at the surface of an aerofoil of non-zero thickness. The downwash at the chord-line of the section was then obtained in the usual way by means of a correction term which takes account of the difference between the downwash at the chord-line and that at the surface. This term is small; it was taken from the theory of the two-dimensional straight aerofoil (*see, e.g.*, Ref. 10, equation (6)). The result of this calculation is called 'exact' in the examples given in Figs. 19 to 21. The downwash was then calculated again from equation (45) for the same vortex distribution $\gamma_x(x)$, and the result plotted as ' approximation.' $\varphi = 45$ deg was taken in all the examples. Fig. 19 shows the results for a constant chordwise load distribution $\gamma_x(x) = 2V_0$, which gives a cambered section on a two-dimensional wing and on the sheared part of a swept wing. According to equation (45), the downwash at the centre should be the same as that at the sheared part except for a constant shift by the amount

$$\frac{1}{2\pi V_0} \pi \tan \varphi \gamma_x(x) = 1$$

in the present example. Comparison with the ' exact ' calculation shows that this is a good approximation.

A useful indication of the accuracy of equation (45) can be obtained by calculating the actual shape of the chord-line of the aerofoil which is associated with a given chordwise vortex distribution. This shape is obtained by integration :

$$z(x) = \int_0^x \frac{v_{z0}(x)}{V_0}\, dx + \text{const} \qquad (48)$$

It is usually cambered and twisted compared with the ' basic ' shape obtained at the sheared part of the wing, as explained in detail in Ref. 4. The integration has been performed for the constant chordwise load distribution and also for the flat-plate distribution and the circular-arc distribution. The results in Figs. 20 and 21 show that the approximation from equation (45) is very satisfactory, considering the magnitude of the ' centre effect '. It may be concluded that equation (45) is a good approximation for the actual downwash induced by any chordwise distribution of spanwise vortices of constant, or nearly constant, strength along the span, at all points along the centre line chord. This method of checking the accuracy of the method of calculation (by comparing the shape of the real wing with that which the assumed vortex distribution does in fact represent) is more severe than merely comparing the final resulting span loadings.

3.2.3. *Experimental Verification.*—The simplest and most direct experimental check on the accuracy of equation (45) is to calculate the downwash for a given vortex distribution from equation (45) and subsequently the shape of the aerofoil from equation (48) and test this aerofoil. This has been done for the flat-plate distribution, equation (2), which gives a symmetrical aerofoil section on the sheared part of the wing and a cambered and twisted section at the centre*, like that in Fig. 21. The measured chordwise load distribution should then be the same at the centre as at the sheared part of the wing, at the design C_L. This was borne out by the experiment. (*see* wing C in Ref. 46.)

Another experimental proof of the reliability of equation (45) can be obtained by considering the normal and tangential forces at the centre-section. Experimental values of C_T and C_N^2 from various spanwise stations on a 45-deg swept-back wing are plotted in Fig. 22. There is still a linear relation between C_T and C_N^2, and at the sheared part of the wing (y/c about 1) the experimental points clearly obey a relation $C_T = -C_N^2/a$ (where $a = a_0 \cos \varphi$), as was found on straight wings. As the centre of the wing is approached, an increase of C_T at $C_N = 0$ is found. This is due to the distortion of the pressure distribution on the surface of the thick aerofoil at zero lift, which has been discussed in detail in Ref. 47. There is, however, another effect at non-zero lift, which appears as a rapid decrease of the slope of the C_T vs. C_N^2 curves as $y \to 0$. At $y = 0$, C_T is practically independent† of C_N. This behaviour can be explained if a downwash equation of the type of equation (45) holds, as will be shown presently.

---

* The shape of this section is given in Refs. 4 and 46.

† That C_T is not exactly constant will be due to the effect of the boundary layer which reduces the lift increment mainly at the rear part of the centre-section and thus reduces C_T.

At the centre-section, the tangential force can be obtained from the Kutta-Joukowski theorem :

$$C_T = -2 \int_0^1 \frac{v_z^*}{V_0} \frac{\gamma_x(x')}{V_0} \, dx' \, . \quad \ldots \quad (49)$$

v_z^* is defined as the principal value of the downwash integral, that is as the resultant downwash induced at the point $x = x'$ by all the vortices except the one passing through $x = x'$, the contribution which the ' vortex element ' at the point $x = x'$ itself might make being excepted. No vortex element contributes to the downwash at its own position if the downwash equation is of the type

$$\frac{v_{z\,0}}{V_0} = \frac{1}{2\pi V_0} \int_0^1 \int_0^\infty \gamma_x(x',y') \, f(x,x',y') \, dx' \, dy' \, . \quad \ldots \quad (50)$$

Thus,

$$\frac{v_{z\,0}}{V_0} = \frac{v_z^*}{V_0} = \alpha_{e\,0} = \frac{C_L}{a} \quad \ldots \quad (51)$$

for an uncambered aerofoil at incidence $\alpha_{e\,0}$. Inserting this value of v_z^* into equation (49), we find

$$C_T = -2 \frac{C_L}{a} \int_0^1 \frac{\gamma_x(x')}{V_0} \, dx' = -\frac{C_L^2}{a} \triangleq -\frac{C_N^2}{a} \, . \quad \ldots \quad (52)$$

This explains the results found at the sheared part of the wing ; but it is obviously not true for the centre-section, as can be seen from Fig. 22, unless a is infinite, which it is not, as will be shown later. Therefore, the downwash equation at the centre-section cannot be of the type of equation (50). If however, the downwash is given by an equation of the type

$$\frac{v_{z\,0}}{V_0} = \frac{1}{2\pi V_0} \left\{ \int_0^1 \int_0^\infty \gamma_x(x',y') \, f(x,x',y') \, dx', \, dy' + \sigma(\varphi,y) \, \gamma_x(x) \right\} , \quad \ldots \quad (53)$$

then the principal value of the downwash integral is

$$\frac{v_z^*}{V_0} = \frac{v_{z\,0}}{V_0} - \frac{\sigma}{2\pi} \frac{\gamma_x(x)}{V_0} = \frac{C_L}{a} - \frac{\sigma}{2\pi} \frac{\gamma_x(x)}{V_0} , \quad \ldots \quad (54)$$

and equation (49) gives

$$C_T = -2 \frac{C_L}{a} \int_0^1 \frac{\gamma_x(x')}{V_0} \, dx' + \frac{\sigma}{\pi} \int_0^1 \left(\frac{\gamma_x(x')}{V_0} \right)^2 dx'$$

$$= -\frac{C_N^2}{a} + \frac{\sigma}{\pi} \int_0^1 \left(\frac{\gamma_x(x')}{V_0} \right)^2 dx' \, . \quad \ldots \quad (55)$$

The correction term is always positive, for $\sigma > 0$ (*i.e.*, for $\varphi > 0$), and thus the thrust is reduced. With the $\gamma_x(x)$ distribution from equation (46),

$$\int_0^1 \left(\frac{\gamma_x(x')}{V_0} \right)^2 dx' = 4 \cos^2 \varphi \, \alpha_{e\,0}^2 \int_0^1 \left(\frac{1-x'}{x'} \right)^{2n_0} dx'$$

$$= \frac{1}{\tan \varphi} \frac{C_N^2}{a} \frac{4\pi n_0}{a} \, .$$

With $\sigma = \pi \tan \varphi$ from equation (45), this gives for the tangential force from equation (55),

$$C_T = -\frac{C_N^2}{a}\left(1 - \frac{4\pi n_0}{a}\right) = 0\,, \qquad (56)$$

since $a = 4\pi n_0$, from Ref. 3. This shows that a downwash equation of the type of equation (45) is needed to explain the striking behaviour of the tangential force, which can be observed at the centre-section of any swept wing.

These results imply that there is really a local drag force at the centre-section of a swept-back wing (and a thrust force at the centre of a swept-forward wing), which is induced by the spanwise vortices. Its magnitude is $C_D = C_N^2/a$), since $C_D = 0$ implies $C_T = -C_N^2/\alpha$ (*see* section 2.2) and Fig. 2). This constitutes a characteristic difference between the centre of a swept wing and straight or sheared wings where no such drag forces occur. In fact, α_e has been interpreted there as giving the direction in which the resultant air force has no component ; this is no longer true near the centre and tips of swept wings (*see* also section 3.7) below.

3.3. *Downwash and Chordwise Loading at any Spanwise Station on Wings of Infinite Aspect Ratio.*—The downwash equation (45) can be generalised to be applicable to any spanwise station y (which is measured in terms of the local chord) by putting :—

$$\frac{v_{z0}}{V_0} = \frac{1}{2\pi V_0}\left\{\int_0^1 \gamma_x(x')\,\frac{dx'}{x - x'} + \sigma(\varphi, y)\,\gamma_x(x)\right\}. \qquad (57)$$

This includes the special case of the centre-line if $\sigma = \pi \tan \varphi$ for $y = 0$; and the two-dimensional straight or sheared wing if $\sigma = 0$ for $y = \infty$. (*see* equation (3).) σ is independent of x at the centre and at the sheared part of the wing ; it is now assumed to be independent of x everywhere. How σ depends on φ and y will be determined later.

A solution of equation (57) for the case $v_{z0}/V_0 = \alpha_{e0} =$ const is again a function of the type

$$\gamma_x(x) = C\left(\frac{1-x}{x}\right)^{n_0}.$$

Inserting this into equation (57), we find

$$\alpha_{e0} = \frac{C}{2\pi V_0}\left\{\frac{\pi}{\sin \pi\, n_0} - \left[\pi \cot \pi\, n_0 - \sigma(\varphi, y)\right]\left(\frac{1-x}{x}\right)^{n_0}\right\}.$$

This gives first

$$\sigma(\varphi, y) = \pi \cot \pi n_0 \qquad (58)$$

to make the right-hand side independent of x. Then

$$C = 2\alpha_{e0}\, V_0 \sin \pi n_0\,,$$

so that the final solution becomes

$$\gamma_x(x) = 2\alpha_{e0} V_0 \sin \pi n_0 \left(\frac{1-x}{x}\right)^{n_0}. \qquad (59)$$

This includes the solution (46) for the centre-line, $y = 0$, where

$$n_0 = \tfrac{1}{2}\left(1 - \frac{\varphi}{\pi/2}\right) \text{ and } \sin \pi\, n_0 = \cos \varphi\,.$$

It also includes the flat-plate distribution for the sheared wing, $y = \infty$, where

$$n_0 = \tfrac{1}{2} \text{ and } \sin \pi n_0 = 1.$$

Thus in general n_0 can be written as

$$n_0 = \tfrac{1}{2}\left(1 - \lambda(y)\,\frac{\varphi}{\pi/2}\right), \qquad (60)$$

where λ is a function of y with $\lambda = 1$ at $y = 0$ and $\lambda = 0$ at $y = \infty$.

The interpolation function $\lambda(y)$ is related to the shift of the aerodynamic centre due to the centre effect

$$\Delta x_{\text{a.c.}} = x_{\text{a.c.}} - \tfrac{1}{4} = \lambda(y)\,\frac{\varphi}{2\pi} \qquad (61)$$

by equations (12) and (60). $\lambda(y)$ need not be determined very accurately since, by equation (61) with $\varphi = \pi/2$ (the extreme case), a certain error in $\lambda(y)$ can lead only to a quarter of that error in $x_{\text{a.c.}}$. In the practical range of sweep angles, an error of 5 per cent in $\lambda(y)$ (which is the difference between the two estimates in Fig. 23) results in an error of about $\frac{1}{2}$ per cent in the position of the aerodynamic centre. Since we are dealing with a physical problem, the locus of the aerodynamic centre along the wing span can be expected to be a continuous line which crosses the centre-line of the wing at right-angles. For a flat wing of infinite span, this locus can reasonably be approximated by a hyperbola with the quarter-chord lines of the two wing halves as asymptotes, *see* Fig. 23. The function $\lambda(y)$ is then, by equation (61),

$$\lambda(y) = \sqrt{\left\{1 + \left(2\pi\,\frac{\tan\varphi}{\varphi}\,y\right)^2\right\}} - 2\pi\,\frac{\tan\varphi}{\varphi}\,y\,, \qquad (62)$$

y being measured in terms of the wing chord. Since the term $\tan\varphi/\varphi$ does not vary very much with sweep, equation (62) may be simplified into

$$\lambda(y) = \sqrt{\{1 + (2\pi y)^2\}} - 2\pi y. \qquad (63)$$

This relation will be sufficiently accurate in most practical cases, and only for very highly swept wings need the complete relation (62) be used, in which λ depends also on φ.

An alternative relation for $\lambda(y)$ can be obtained by assuming the aerodynamic centre positions to lie on the envelope of a series of inter sections as shown in Fig. 23, in which case the aerodynamic centre locus runs tangentially into the quarter-chord line at a given finite distance y. Taking this distance as $y = 1$ gives

$$\lambda(y) = 1\cdot 40 + 1\cdot 33y - \sqrt{(0\cdot 16 + 7\cdot 30y)}\,. \qquad (64)$$

This relation has been used in Ref. 3, Fig. 1. Both relations (63) and (64) are plotted in Fig. 23, and it can be seen that the difference between them is very small and of no practical significance, although they have been derived from extremely different assumptions. These relations are supported by experimental data (further results from tests are shown in Ref. 3, Fig. 1). With the function $\lambda(y)$ known, n_0 can be determined from equation (60), and subsequently the chordwise vortex distribution from equation (59), and the value of σ in equation (57) from equation (58).

The vortex distribution $\gamma_x(x)$ is not the same as the chordwise load distribution $\Delta C_p(x)$, except in special cases where the vortex lines are normal to the main stream ; *e.g.*, at the centre, $y = 0$, where

$$\Delta C_p(x) = -\,2\,\frac{\gamma_x(x)}{V_0}$$

as on a straight wing, equation (2). On the sheared part of the wing,

$$\Delta C_p(x) = -\,2\cos\varphi\,\frac{\gamma_x(x)}{V_0}\,,$$

and in general

$$\Delta C_p(x) = -\,2\cos\varphi_v\,\frac{\gamma_x(x)}{V_0}\,, \qquad (65)$$

where φ_v is the direction of the vorticity vector (not that of its component $\gamma_x(x)$ which is φ except at the centre-line), as explained in detail in Ref. 4. $\varphi_v = 0$ at all points on the centre-line; $\varphi_v = \varphi$ at all points along the chord of a section on the sheared part of the wing. But at intermediate spanwise stations φ_v may depend on x. It is, however, not necessary to know very accurately how φ_v varies between 0 and φ, since again only second-order terms are involved. Therefore, any possible variation of φ_v with x may be ignored and φ_v may be replaced by a mean value across the chord. φ_v could then be taken as the sweep of the aerodynamic centre-line which was assumed to be a hyperbola. Hence,

$$\cos^2 \varphi_v = \frac{1 + \left(2\pi \dfrac{\tan \varphi}{\varphi} y\right)^2}{1 + (1 + \tan^2 \varphi)\left(2\pi \dfrac{\tan \varphi}{\varphi} y\right)^2} \simeq \frac{1 + (2\pi y)^2}{1 + (1 + \tan^2 \varphi)(2\pi y)^2} \quad \ldots \quad (66)$$

y being measured in terms of the wing chord. For practical purposes, it is usually sufficiently accurate to replace equation (66) by the simpler relation

$$\cos \varphi_v = \frac{\cos \varphi}{\cos \lambda\varphi} = \frac{\cos \varphi}{\sin \pi n_0}, \quad \ldots \quad (67)$$

as suggested in Ref. 4. The general expression for the chordwise loading at any spanwise station of a swept wing of infinite aspect ratio is then, using equations (59), (65) and (67),

$$\Delta C_p(x) = -4\alpha_{e0} \cos \varphi \left(\frac{1-x}{x}\right)^{n_0}. \quad \ldots \quad (68)$$

An alternative derivation of equation (67) to that given in Ref. 4 can be obtained as follows: Equation (68) is known to apply both at the sheared wing and at the centre-section. The only difference between the chordwise loadings at the two places is that n_0 has a different value at each, namely $n_0 = \frac{1}{2}$ at the sheared wing and $n_0 = \frac{1}{2}(1 - \varphi/\frac{1}{2}\pi)$ at the centre-section. We now proceed on the assumption that equation (68) applies at all stations between the centre and the sheared part and that only n_0 depends on the spanwise co-ordinate y. If this were not so, there would have to be another function of y in the expression for ΔC_p, which would be unity at the centre and sheared part but would have other values in between. This is unlikely. Applying equation (65) in which φ_v is the mean sweep over the chord of the vorticity vector, and which follows immediately from the Kutta-Joukowsky theorem, we find

$$\frac{\gamma_x(x)}{V_0} = 2\alpha_{e0} \frac{\cos \varphi}{\cos \varphi_v} \left(\frac{1-x}{x}\right)^{n_0}$$

at any intermediate station. Inserting this function into the general downwash equation (57), with σ from equation (58),

$$\frac{v_{z0}}{V_0} = \alpha_{e0} = \frac{1}{\pi} \alpha_{e0} \frac{\cos \varphi}{\cos \varphi_v} \left\{\frac{\pi}{\sin \pi n_0} - \left(\frac{\pi}{\tan \pi n_0} - \pi \cot \pi n_0\right)\left(\frac{1-x}{x}\right)^{n_0}\right\}$$

which gives

$$\cos \varphi_v = \frac{\cos \varphi}{\sin \pi n_0}$$

as before.

3.4. *Determination of the Sectional Lift Slope.*—By equation (5), the local lift coefficient, $C_L(\eta)$, at any spanwise station $\eta = 2yc/b$ is obtained by integrating $\Delta C_p(x)$ over the chord. For the chordwise loading given by equation (68),

$$C_L = -\int_0^1 \Delta C_p(x)\, dx = 4\alpha_{e0} \cos \varphi \int_0^1 \left(\frac{1-x}{x}\right)^{n_0} dx = 4\alpha_{e0} \cos \varphi \frac{\pi n_0}{\sin \pi n_0}.$$

The sectional lift slope at any spanwise station on a swept wing of infinite aspect ratio is then

$$\frac{C_L}{\alpha_{e0}} = \frac{4\pi n_0 \cos\varphi}{\sin \pi n_0}, \quad \ldots \quad (69)$$

giving

$$\frac{C_L}{\alpha_{e0}} = 2\pi\left(1 - \frac{\varphi}{\pi/2}\right) \quad \ldots \quad (70)$$

for the centre-section, $y = 0$; and

$$\frac{C_L}{\alpha_{e0}} = 2\pi \cos\varphi \quad \ldots \quad (71)$$

for the sheared wing, using equation (60) for the values of n_0. These relations have already been derived in Ref. 3. Replacing α_{e0} in equation (68) by C_L from equation (69), we find for the chordwise loading

$$\Delta C_p(x) = -\frac{\sin \pi n_0}{\pi n_0} C_L \left(\frac{1-x}{x}\right)^{n_0}, \quad \ldots \quad (72)$$

and for the chordwise vortex distribution

$$\frac{\gamma_x(x)}{V_0} = \frac{\sin^2 \pi n_0}{2\pi n_0 \cos\varphi} C_L \left(\frac{1-x}{x}\right)^{n_0}, \quad \ldots \quad (73)$$

by equation (59).

The chordwise loading on a swept wing of infinite aspect ratio from equation (72) is of the same type as the chordwise loading on a straight wing of any aspect ratio, which is given by equation (11). We assume, therefore, that the chordwise loading on a swept wing of any aspect ratio is also of the same type :

$$\Delta C_p(x) = -\frac{\sin \pi n}{\pi n} C_L \left(\frac{1-x}{x}\right)^{n}, \quad \ldots \quad (74)$$

where n will depend on the aspect ratio of the wing and on φ and y. $n = n_0$ for $A \to \infty$. The generalised vortex distribution is then, by equations (65) and (67),

$$\frac{\gamma_x(x)}{V_0} = \frac{\sin \pi n_0 \sin \pi n}{2\pi n \cos\varphi} C_L \left(\frac{1-x}{x}\right)^{n}. \quad \ldots \quad (75)$$

We can now determine the effective incidence, α_e, which is induced by the spanwise vortices on a swept wing of any aspect ratio on the basis of our general hypothesis by inserting v_{z0}/V_0 from equation (57) into equation (44), with $\gamma_x(x)$ from equation (75) as the chordwise distribution. This gives

$$\alpha_e = \frac{C_L}{2\pi}\frac{\sin \pi n_0 \sin \pi n}{2\pi n \cos\varphi}\int_0^1 \left\{\frac{\pi}{\sin \pi n} - \left[\pi \cot \pi n - \pi \cot \pi n_0\right]\left(\frac{1-x}{x}\right)^n\right\} dx$$

$$= C_L \frac{\sin \pi n_0}{4\pi n \cos\varphi}\left\{1 - \pi n(\cot \pi n - \cot \pi n_0)\right\}, \quad \ldots \quad (76)$$

so that

$$a = \frac{C_L}{\alpha_e} = 2\pi \frac{\cos\varphi}{\sin \pi n_0} \frac{2n}{1 - \pi n(\cot \pi n - \cot \pi n_0)},$$

or, replacing the two-dimensional lift slope by a_0,

$$a = a_0 \frac{\cos \varphi}{\sin \pi n_0} \frac{2n}{1 - \pi n(\cot \pi n - \cot \pi n_0)} . \qquad (77)$$

This relation includes as special cases all the expressions for the sectional lift slope previously derived. For instance, for a straight wing, $n_0 = \frac{1}{2}$ by equation (60), which leads to equation (13). Again, for a swept wing of infinite aspect ratio, $n = n_0$, which leads to equation (69). For the sheared part of a swept wing of finite aspect ratio, $n_0 = \frac{1}{2}$ again, so that the sectional lift slope there is

$$a_S = a_0 \frac{2n_S \cos \varphi}{1 - \pi n_S \cot \pi n_S} , \qquad (78)$$

where n_S denotes the corresponding value of n, which will be determined later.

The change of the sectional lift slope due to the effects of aspect ratio, sweep, and spanwise position may be regarded as a change of the effective incidence which is needed to produce a certain lift at that aerofoil section. Whereas, for a straight two-dimensional aerofoil in inviscid flow, an incidence $\alpha_{ep} = C_L/2\pi$ produces the lift coefficient C_L, a different incidence, $\alpha_e = C_L/a$ is needed in the general case. The ratio between the two is

$$\frac{\alpha_{ep}}{\alpha_e} = \delta = \frac{\cos \varphi}{\sin \pi n_0} \frac{2n}{1 - \pi n(\cot \pi n - \cot \pi n_0)} , \qquad (79)$$

by equation (77). This relation must be used if the pressure distribution on the surface of an aerofoil of non-zero thickness is calculated by means of a method which is basically derived for two-dimensional straight aerofoils, such as the method in Ref. 10. All incidences occurring in such methods are really values α_{ep} and they must be replaced by $\alpha_e\delta = (\alpha - \alpha_i)\delta$.

3.5. *The Spanwise Load Distribution.*—As explained in section 3.1, the span loading equation for a swept wing is the same as that for a straight wing, namely equation (15). The two main differences are: that the sectional lift slope on a swept wing depends not only on the aspect ratio but also on the angle of sweep and on the spanwise co-ordinate; and that the value of the parameter n is affected by sweep. In general, the changes due to sweep do not affect the calculation procedure, and Multhopp's method[17] can be applied, equation (16). In determining the sectional lift slope a, the wing tips are assumed to behave like the centre of a wing of opposite sweep, as explained in Ref. 3.

The downwash factor ω in equation (16) is still assumed to be equal to $2n$, but it is assumed that ω/n does not vary along the span, as n does. It is therefore proposed to use a mean value of n here. The value, n_S, at the sheared part of the wing is suitable for the present purpose, so that $\omega = 2n_S$. Relations for n and n_S will be derived in section 3.6. The 'sheared part' of the wing can be defined more precisely here as that part of the span where $\lambda = 0$. There is always at least one station where $\lambda = 0$, even if the aspect ratio is so small that centre and tip effects overlap.

For swept wings of large aspect ratio, $n \rightarrow n_0$, and the method reduces to that given in Ref. 3, which may be regarded as the equivalent of Prandtl's aerofoil theory in the case of a swept wing. For swept wings of very small aspect ratio, the plan-form term

$$\frac{2b}{ac} = \frac{2}{a.c/\bar{c}} A$$

in equation (15) is small compared with α and can be ignored in the limit $A \rightarrow 0$. Thus the considerations of section 2.2 apply again. In particular, the span loading becomes elliptic, equation (19), and the overall lift coefficient is $C_L/\alpha = \pi A/2$, by equation (20), for swept wings also. These results agree with those of R. T. Jones[2].

To obtain elliptic span loading with wings of moderate or large aspect ratios, a certain plan-form is required, where the chord does not decrease elliptically towards the tips, as explained in Ref. 3. However, the overall lift coefficient of wings with elliptic span loading can still be obtained from equation (21) if a is replaced by the value, a_S, at the sheared part of the wing. Thus,

$$\frac{\bar{C}_L}{\alpha} = \frac{1}{\dfrac{1}{a_S} + \dfrac{\omega}{\pi A}} = \frac{2a_0 n_S \cos\varphi}{1 - \pi n_S \cot \pi n_S + \dfrac{4a_0 n_S{}^2 \cos\varphi}{\pi A}}, \quad \ldots \quad \ldots \quad \ldots \quad (80)$$

putting $\omega = 2n_S$. This relation differs from equation (21) in that the two-dimensional lift slope a_0 is replaced by $a_0 \cos\varphi$ (or $2\pi \cos\varphi$), *i.e.*, by the sectional lift slope of the infinite sheared wing. We may, therefore, extend Helmbold's formula (29) in the same manner, although its derivation is even less justifiable for swept wings. This gives

$$\frac{\bar{C}_L}{\alpha} = \frac{a_0 \cos\varphi}{\sqrt{\left\{1 + \left(\dfrac{a_0 \cos\varphi}{\pi A}\right)^2\right\}} + \dfrac{a_0 \cos\varphi}{\pi A}}, \quad \ldots \quad \ldots \quad \ldots \quad \ldots \quad \ldots \quad (81)$$

which has already been suggested by F. W. Diederich[31] who has shown that reasonable estimates can be obtained, in particular for delta wings of small aspect ratio. This can be expected also from the considerations in Ref. 3 where it was shown that swept-back wings must be highly tapered in order to give elliptic span loading. For delta wings with pointed tips and straight trailing edge,

$$\cos\varphi = \cos\varphi_{c/2} = \frac{A}{\sqrt{(4 + A^2)}},$$

so that

$$\frac{\bar{C}_L}{\alpha} = \frac{a_0 A}{\sqrt{\left\{4 + A^2 + \left(\dfrac{a_0}{\pi}\right)^2\right\}} + \dfrac{a_0}{\pi}},$$

by equation (81). This relation is confirmed by experiments (*see e.g.*, Ref. 20) for such wings, up to an aspect ratio of about 2·5.

3.6. *Determination of the Parameter n.*—A general relation for the parameter n is derived by considering the values it must have in the extreme cases of very low and of very high aspect ratio, as was done in section 2.2 for straight wings. We know already that n approaches the value n_0 from equation (60) for swept wings of very large aspect ratio. At low aspect ratios, where the span loading tends to be elliptical, equation (80) can be used for the overall lift coefficient which must be equal to $\pi A/2$. Thus

$$\frac{\pi A}{2} = \frac{4\pi n_S \cos\varphi}{1 - \pi n_S \cot \pi n_S + \dfrac{8n_S{}^2 \cos\varphi}{A}}$$

for $a_0 = 2\pi$. This gives

$$n_S = 1 - \sqrt{\left(\frac{A}{8\cos\varphi}\right)} \to 1 \quad \text{as} \quad A \to 0, \quad \ldots \quad \ldots \quad \ldots \quad \ldots \quad (82)$$

if $\varphi =$ const. The sectional lift slope is then, by equation (78),

$$a_S = 2\pi \cos\varphi \sqrt{\left(\frac{A}{2\cos\varphi}\right)} \to 0 \quad \text{as} \quad A \to 0, \quad \ldots \quad \ldots \quad \ldots \quad \ldots \quad (83)$$

and the effective incidence

$$\frac{\alpha_e}{\alpha} = \sqrt{\left(\frac{A}{8 \cos \varphi}\right)} \to 0 \quad \text{as} \quad A \to 0 . \qquad \ldots \quad \ldots \quad \ldots \quad \ldots \quad \ldots \qquad (84)$$

These relations correspond to equations (22), (23) and (24) for the case of unswept wings. They are again consistent with R. T. Jones's results. The only change due to sweep is that the aspect ratio A is replaced by $A/\cos \varphi$ in all three relations.

On this basis, equation (25) for n may be generalised to

$$n_S = 1 - \frac{1}{2\left\{1 + \left(\frac{a_0 \cos \varphi}{\pi A}\right)^2\right\}^{1/4}} . \qquad \ldots \quad \ldots \quad \ldots \quad \ldots \quad \ldots \qquad (85)$$

The main consequence of the term $A/\cos \varphi$ is that small aspect ratio effects become important only at smaller values of A on swept wings than on straight wings. Whereas Prandtl's classical aerofoil theory fails for straight wings of aspect ratios below about 6, the ' large aspect ratio theory ' of Ref. 3 holds down to aspect ratios of about 3 in the normal sweep range.

The results so far obtained apply to wings of varying aspect ratio but with constant angle of sweep. In reality, the effective sweep begins to differ from the geometric sweep when the aspect ratio of the wing becomes very small. This can be explained as follows: On a wing of large aspect ratio, a large part of the span can be considered as having the properties of an infinite sheared wing, the sweep of the spanwise vortices being the same as the geometric sweep. Distortions occur only near the centre and near the tips, the vortex lines curving back towards the rear of the section near the centre, and curving forward towards the leading edge near the tips. If the aspect ratio of the wing is reduced, the centre and tip distortions will gradually merge. As a consequence, the aerodynamic centre line, and thus the angle of sweep of the vorticity vector, φ_v, will never attain the full geometric sweep if the aspect ratio is small, φ_v being zero at the centre and at the tips anyway. This means that an ' effective angle of sweep,' φ_e, should be introduced which becomes gradually smaller than the geometric angle of sweep, $\varphi_{c/2}$, as the aspect ratio is reduced*. Very little is known about this effect and only suggestions can be made at this stage. A reasonable approximation is

$$\varphi_e = \frac{\varphi_{c/2}}{\left\{1 + \left(\frac{a_0 \cos \varphi_{c/2}}{A\pi}\right)^2\right\}^{1/4}} , \qquad \ldots \quad \ldots \quad \ldots \quad \ldots \quad \ldots \qquad (86)$$

which has been derived by an iteration process. The sweep of the straight line joining the aerodynamic centre positions at the centre and the tips on untapered wings was determined first; new aerodynamic centre positions were then calculated, using the new, reduced, sweep, and the sweep of the straight line joining these obtained; and so on. For very small aspect ratios,

$$\varphi_e = \varphi \sqrt{\left(\frac{A}{2 \cos \varphi}\right)} \to 0 \text{ as } A \to 0 . \qquad \ldots \quad \ldots \quad \ldots \quad \ldots \quad \ldots \qquad (87)$$

It is proposed to use the effective sweep from equation (86) instead of the geometric sweep of the mid-chord line in all relations wherever φ occurs.

With the effective sweep tending to zero as $A \to 0$, the limiting relation (82) for n_S is still fulfilled if equation (85) is replaced by

$$n_S = 1 - \frac{1}{2\left\{1 + \left(\frac{a_0 \cos \varphi}{\pi A}\right)^2\right\}^{\frac{1}{4(1 + |\varphi|/\frac{1}{2}\pi)}}} . \qquad \ldots \quad \ldots \quad \ldots \quad \ldots \qquad (88)$$

* The introduction of an effective angle of sweep does not imply, however, that there can no longer be a station which behaves like a ' sheared ' wing. There is always a station, near mid-semispan, where $\lambda = 0$ and $n = n_S$.

The condition $n_S \to n_0 = \frac{1}{2}$ for large aspect ratios is also fulfilled. The change of the exponent from $\frac{1}{4}$ to

$$\frac{1}{4(1 + |\varphi|/\frac{1}{2}\pi)},$$

where $|\varphi|$ denotes the modulus of φ, appears desirable from practical experience and is thus empirical. The change has only a small effect. Further work is needed to settle this point satisfactorily.

With n_S being known, the value of the downwash factor ω can be determined. Since $\omega = 2n_S$.

$$\omega = 2 - \frac{1}{\left\{1 + \left(\frac{a_0 \cos \varphi}{\pi A}\right)^2\right\}^{\frac{1}{4(1 + |\varphi|/\frac{1}{2}\pi)}}} . \qquad (89)$$

For large aspect ratios, $\omega \to 1$ as $A \to \infty$; for small aspect ratios,

$$\omega = 2 - \sqrt{\left(\frac{A}{2 \cos \varphi}\right)} \to 2 \quad \text{as} \quad A \to 0 \qquad (90)$$

by equation (82).

We still have to find a general expression for the value of n at any spanwise station on a swept wing. We take the spanwise variation of n for any aspect ratio as being the same as obtained by the superposition of wings of large aspect ratio, which is given by equation (60) ; and we take the variation with aspect ratio for any spanwise station as being the same as that for the sheared part of the wing, which is given by equation (88). This leads to

$$n = 1 - \frac{1 + \lambda(y) \dfrac{\varphi}{\pi/2}}{2\left\{1 + \left(\frac{a_0 \cos \varphi}{\pi A}\right)^2\right\}^{\frac{1}{4(1 + |\varphi|\frac{1}{2}\pi)}}}, \qquad (91)$$

which contains all the relations for n deduced so far as special cases. $\lambda(y)$ is the interpolation function which was discussed in section 3.3. The magnitude of $\lambda(y)$ can be determined from equations (63) or (64) or from Fig. 1 in Ref. 3. y is to be measured in terms of the local chord either from the centre-line of the wing $y = y_C$ (for the centre region), or from the tips, $y = y_T$ (for the tip regions). $\lambda(y)$ is negative in the tip regions, because the tip behaves like the centre of a wing of opposite sweep, *see* Ref. 3. $\lambda = +1$ at the centre ; $\lambda = -1$ at the tips ; $\lambda = 0$ on the sheared part of the wing. At intermediate stations,

$$\lambda(y) = \lambda(y_C) + \lambda(y_T) = \lambda_C + \lambda_T . \qquad (92)$$

This relation may be interpreted in physical terms as being only another statement of the general hypothesis used throughout. The conditions at any spanwise station are obtained from the superposition of three terms :

(i) A basic term which does not include centre and tip effects, *i.e.*, with $\lambda = 0$. This is essentially the same as that for an unswept wing of the same aspect ratio except for a change of the two-dimensional lift slope from a_0 to $a_0 \cos \varphi$.

(ii) An additional term which takes account of the centre effect. This is obtained from a fictitious untapered wing which has the same sweep and chord as the section considered, with the central kink at the same position as on the real wing ; *i.e.*, the kink is at a given distance y_C/c from the station considered.

(iii) A third term which takes account of the tip effect. This is obtained from another fictitious untapered wing, of infinite semi-span, which has the same sweep and chord as the station considered and with its tip at the same position as on the real wing ; *i.e.*, the tip is at a given distance y_T/c from the station considered.

Centre and tip effects will overlap if the aspect ratio is small enough with the twofold effect that the effective sweep is reduced and the centre and tip effects reduce each other as compared with those on a wing of large aspect ratio where they do not merge.

The general calculation procedure can now be described as follows: For a given wing, the values of A, $\varphi_{c/2}$, and a_0 are known. The effective sweep, φ_e, is then determined from equation (86) and its value inserted into equation (91) to find n at any spanwise station, where $\lambda(y)$ is obtained from equations (92) and (63) or (64). With n known, values of the sectional lift slope are found from equation (77) and the downwash factor from equation (89). The spanwise loading is then determined by solving equation (16), and subsequently the chordwise loading at any spanwise station is found from equation (74). The chordwise position of the aerodynamic centre at any spanwise position is given by equation (12).

3.7. *Drag*.—The induced drag of swept wings can be calculated in the same way as has been explained in section 2.5. In particular, the minimum induced drag is given by the well-known relation (36) for wings with elliptic span loading, whether the wing is swept or not. However, the wing plan form which gives minimum induced drag is not elliptic if the wing is swept[3]. This implies that a swept-back wing can have the same induced drag as a wing of the same aspect ratio swept forward by the same amount ('reversibility theorem,' *see*, *e.g.*, Refs. 49, 50); but their plan forms must be different to achieve this: the swept-back wing must be highly tapered, whereas the swept-forward wing must have little or no taper, or possibly inverse taper, depending on the amount of sweep.

The main effect of sweep is to produce local drag forces in the centre region of swept-back wings and thrust forces near their tips, as has been described in Ref. 51. These forces cancel each other on the wing as a whole, but their local values may be very high. The thrust forces near the tips usually cause increased leading-edge suctions peaks and are, therefore, responsible for the unpleasant stalling characteristics of swept-back wings and also for the premature occurrence of shock-waves at high Mach numbers.

The local drag force at a spanwise station η can be written as

$$C_D(\eta) = C_{Di}(\eta) + C_L\alpha_e + C_T + C_{DF} . \qquad \ldots \qquad (93)$$

C_{Di} is the local induced drag which is obtained from the relation

$$C_{Di}(\eta) = C_L(\eta)\,\alpha_{i0}(\eta) = \frac{1}{\omega} C_L(\eta) \left[\alpha(\eta) - \frac{C_L(\eta)}{a(\eta)}\right] , \qquad \ldots \qquad (94)$$

using equations (9) and (37). $C_L\alpha_e$ can be replaced by $C_L{}^2/a$. C_{DF} measures the form drag and skin friction, *i.e.*, the viscosity effects. C_T is the tangential force coefficient which has been discussed in section 3.2.3. Normally, *i.e.*, on straight wings and outside the influence of centre and tip on swept wings, $C_T = -C_L\alpha_e$. In that case, the drag at any spanwise station consists of induced drag C_{Di} and skin friction and form drag C_{DF}. However, $C_T = 0$ at the centre-section by equation (56), so that a drag force, $C_L{}^2/a$, remains there and a corresponding thrust force, $-C_L{}^2/a$, at the tips.

The tangential force at any spanwise station can be determined from the Kutta-Joukowski theorem as:

$$C_T = -2\int_0^1 \cos\varphi_v(x')\,\frac{v_z{}^*}{V_0}\,\frac{\gamma_x(x')}{V_0}\,dx' , \qquad \ldots \qquad (95)$$

which is the generalisation of equation (49) for the special case $\varphi_v = 0$. This integral cannot easily be evaluated because the sweep, φ_v, of the vorticity vector cannot be assumed independent of x for this purpose where quadratic terms are concerned. Experimental evidence suggests that

$$C_T = -\frac{C_L{}^2}{a(\eta)}\,(1 - \lambda(\eta)) , \qquad \ldots \qquad (96)$$

at least for wings of large aspect ratio. An example is given in Fig. 22. Equation (96) gives $C_T = 0$ at $y = 0$, in accordance with equation (56); and $C_T = - C_L^2/a$ for two-dimensional wings, in accordance with equation (8). Combining equations (93) and (96), we obtain

$$C_D(\eta) = C_{Di}(\eta) + \lambda(y) \frac{C_L^2(\eta)}{a(\eta)} + C_{DF} \quad \ldots \quad (97)$$

as the final expression for the local drag coefficients.

3.8. *Non-linear Lift Effects.*—The method for calculating the lift, as described so far, gives the lift at small incidences (*i.e.*, in the limit as $C_L \to 0$) because it is based on linear theory. Non-linear effects occur due to the presence of the tip vortex, even in an otherwise inviscid flow. There is no essential difference between the effects of the tip vortex on straight and swept wings, and the method explained in section 2.6 for assessing these effects can be applied again. The only change required concerns equations (38) and (39) which apply only to straight wings. Since these are based on Helmbold's relation (29), the corresponding relation (81) for swept wings may now be used, which gives

$$\frac{\bar{C}_L}{\alpha} = \frac{a_0 \cos\varphi}{\sqrt{\left\{1 + \left(\varkappa \dfrac{a_0 \cos\varphi}{\pi A}\right)^2\right\}} + \varkappa \dfrac{a_0 \cos\varphi}{\pi A}} \quad \ldots \quad (98)$$

instead of equation (38), and

$$\frac{\bar{C}_L}{\bar{C}_{L0}} = \frac{\sqrt{\left\{1 + \left(\dfrac{a_0 \cos\varphi}{\pi A}\right)^2\right\}} + \dfrac{a_0 \cos\varphi}{\pi A}}{\sqrt{\left\{1 + \left(\varkappa \dfrac{a_0 \cos\varphi}{\pi A}\right)^2\right\}} + \varkappa \dfrac{a_0 \cos\varphi}{\pi A}} \quad \ldots \quad (99)$$

instead of equation (39). How the height of the tip vortex is affected by sweep is not yet known. Equation (43) was derived from experiments on an untapered 45-deg swept-back wing with curved leading edge. (*see* Ref. 41.) It appears that there is no appreciable difference between straight and swept wings in this respect.

3.9. *Examples.*—A few calculated examples will be given to illustrate the magnitude of the small aspect ratio effects and to compare the results with those from experiments and from other calculation methods.

Fig. 24 shows measured and calculated span loadings and centre of pressure positions for a series of untapered 45-deg swept-back wings of various aspect ratios, from Ref. 51. It was on these wings that the limitations of the theory of Ref. 3 first became apparent. Comparing the new results (full lines) with those from Ref. 3 (dotted lines), we find that small aspect ratio effects become noticeable on the wing of aspect ratio 3; they are appreciable for the wing of aspect ratio 2. The results from the new method agree with the experimental results in the whole aspect ratio range tested, from 2 to ∞.

There is good agreement with the results of Multhopp's method[27] and of Falkner's method[23] for moderately tapered wings of about 45-deg sweepback in the aspect ratio range between 2 and 4. In other cases, however, slight differences between the various theoretical results are found. Fig. 25 gives a typical example of how the results of the present theory compare with those of other theories in the case of a wing of fairly large aspect ratio, and Fig. 26 gives a similar typical comparison for a delta wing. On the whole, the present results agree best with Multhopp's method[27]. There is a slight tendency in Multhopp's method to give more pronounced centre and tip effects; the deviation is greatest in the extreme cases of highly tapered wings, where the centre region occupies a large part of the wing area ; and of wings of very large aspect ratio, where the lift changes occur mainly in the centre region and near the tips. This may be related to the fact that Multhopp does not consider the given wing plan form but another wing which has been rounded off in the central region. In cases where experimental results are available, these appear to support the present theory (*see, e.g.*, Figs. 24, 25). In most practical cases of wings of moderate taper and aspect ratio, however, Multhopp's method gives nearly the same answers as the present method. A similar, and usually stronger, tendency to emphasise the centre effect is found in the results of Falkner's method[23], Figs. 24, 25 and 26 ; and this tendency is stronger still in Weissinger's method[21, 52], Fig. 25. This method is based on the three-quarter chord theorem, the application of which to swept wings is even less justifiable than the application to straight wings discussed in section 2.4. In the example given in Fig. 25, Weissinger's results differ from the experiment more than seems permissible.

Measured and calculated span loadings for two highly tapered wings of small aspect ratio are compared in Fig. 27. The agreement is good. When the same wings were discussed in Ref. 3, it was recommended that the distance y_T from the tip, measured in terms of the tip chord, should be used in calculating the interpolation function $\lambda(y)$ and the sectional lift slope. This was to allow (mistakenly) for what is really a low aspect ratio effect. It is not now necessary, and agreement with the experimental results is obtained if the method is applied as explained above (calculation No. I). The results which are obtained by using the tip chord are also shown (calculation No. II) to illustrate the differences which arise from using either the local chord or the tip chord. In the latter case, there is no tip effect at all on a wing with pointed tip (wing A0 in Fig. 27) ; this is physically unsatisfactory since no thrust forces will occur to balance the drag in the central region. On a cropped delta wing (A2 in Fig. 27), a small tip effect exists, which fades out quickly and does not reach the centre. Using the local chord, however, to be consistent with our general hypothesis, there is a tip effect on each wing, which spreads over the whole wing right up to the centre-line. The actual differences in the final results are very small. On wing A0, the value of λ at the centre is reduced by 6 per cent—from $1 \cdot 0$ (calculation II) to $0 \cdot 94$ (calculation I)—but there is no change in the position of the aerodynamic centre ($x_{a.c.}/c = 0 \cdot 329$ for calculation II and $0 \cdot 328$ for calculation I at $y = 0$) ; the overall lift slope is increased by about 3 per cent. On wing A2, there is a reduction of $\lambda(0)$ by 15 per cent—from $1 \cdot 0$ (calculation II) to $0 \cdot 85$ (calculation I) ; this changes the position of the aerodynamic centre by 1 per cent from $x_{a.c.}/c = 0 \cdot 29$ (calculation II) to $0 \cdot 28$ (calculation I) at $y = 0$—and the overall lift slope is increased by about 2 per cent. Experimental results are nearer to those of calculation I, as would be expected, and there is no need to revise the present theory in this respect ; particularly as this question arises only in exceptional cases where high taper is combined with small aspect ratio.

Figs. 28 and 29 show that the chordwise loading too can be estimated with good accuracy by the present method. The magnitude of the small aspect ratio correction can also be seen (the curve marked ' without aspect ratio correction ' has been calculated by the method of Ref. 3). The calculated curves take account of the thickness of the aerofoil section ; the method of Ref. 10 has been used. Fig. 29 illustrates how non-zero thickness and viscosity effects affect the chordwise loading. We begin with the loading of the thin wing in inviscid flow at an incidence which is equal to the given geometric incidence, curve (a) ; the effect of the streamwise vortices is then to reduce the incidence by the amount α_i, which leads to curve (b) ; curve (c) is obtained by taking the thickness of the section ($t/c = 0 \cdot 12$) into account by means of the method of Ref. 10 ; and, finally, the effect of viscosity is calculated from Preston's method[55] by using measured values of the displacement thickness of the boundary layer, as explained in Ref. 11, curve (d). This final result of the calculation agrees with the measured values. The example demonstrates that the effects of aerofoil thickness and viscosity are quite distinct and cannot easily be confused as is sometimes supposed. Further, it may be noted that the methods of Refs. 10 and 55 lead to reasonable results in spite of the fact that both apply basically only to two-dimensional aerofoils but are applied here to a section of a three-dimensional wing. This means that even in these cases it is justifiable to apply our general hypothesis that the properties of an aerofoil section on a three-dimensional wing can be determined by assuming the section to be part of a two-dimensional wing, even though the neighbouring sections may have different properties.

4. *Effects of Compressibility.*—4.1. *The Method Using an Analogous Wing.*—The lift on wings at sub-critical Mach numbers can be conveniently calculated by applying the Prandtl-Glauert analogy in the form of the streamline analogy of Busemann[57] and Gothert[58]. Refinements of the Prandtl-Glauert procedure differ by terms containing the pressure coefficient in incompressible flow, C_{pi}, (*see, e.g.*, Refs. 59 and 60.) Since we are considering thin wings at small incidences, C_{pi} will be small and, therefore, such refinements need not be taken into account when calculating the basic lift term from linear theory.

According to the Prandtl-Glauert analogy, the velocity increment in the direction of the main stream in compressible flow is $1/\beta^2$ times the velocity increment in incompressible flow on an analogous wing obtained by reducing the lateral dimensions of the given wing in the ratio $\beta : 1$.

$\beta = \sqrt{(1 - M_0^2)}$, where M_0 is the free-stream Mach number.

Span, aspect ratio, and angle of sweep of the analogous wing (suffix a) are different from those of the given wing :

$$b_a = \beta b \; ; \; \eta_a = \eta \; ; \; A_a = \beta_A \; ; \cos \varphi_a = \frac{\beta \cos \varphi}{\sqrt{(1 - M_0^2 \cos^2 \varphi)}} . \quad \ldots \quad \ldots \quad (100)$$

The incidence is also reduced :

$$\alpha_a = \beta \alpha . \quad \ldots \quad \ldots \quad (101)$$

The values of the parameter n, of the downwash factor ω, and of the sectional lift slope a must be determined for the analogous wing plan form. The properties of the given wing in compressible flow are then obtained as follows : According to the rule for the velocity increments, the lift coefficient is :

$$C_L = \frac{C_{La}}{\beta^2} ; \; \frac{C_L}{\alpha} = \frac{1}{\beta} \frac{C_{La}}{\alpha_a} ; \; a = \frac{1}{\beta} a_a \quad \ldots \quad \ldots \quad (102)$$

and thus

$$\gamma = \frac{C_L c}{2b} = \frac{\gamma_a}{\beta} , \quad \ldots \quad \ldots \quad (103)$$

and

$$\frac{\gamma}{\alpha} = \frac{\gamma_a}{\alpha_a} . \quad \ldots \quad \ldots \quad (104)$$

Hence, for the overall lift coefficient,

$$\frac{\bar{C}_L}{\alpha} = A \int_{-1}^{+1} \frac{\gamma(\eta)}{\alpha} \, d\eta = A \int_{-1}^{+1} \frac{\gamma_a(\eta_a)}{\alpha_a} \, d\eta_a . \quad \ldots \quad \ldots \quad (105)$$

Since the x-co-ordinate is not affected by the transformation into the analogous wing, the aerodynamic centre position found for any spanwise station on the analogous wing can be taken directly to be that for the corresponding station on the given wing :

$$\frac{x_{\text{a.c.}}(\eta)}{c} = \frac{x_{\text{a.c.}}(\eta_a)}{c} = \frac{1 - n_a(\eta_a)}{2} , \quad \ldots \quad \ldots \quad (106)$$

by equation (12). The chordwise load distribution at any spanwise station of the given wing in compressible flow is :

$$\Delta C_p(x) = - \frac{1}{\beta^2} \frac{\sin \pi n_a(\eta_a)}{\pi n_a(\eta_a)} C_{La}(\eta_a) \left(\frac{1 - x}{x} \right)^{n_a(\eta_a)} . \quad \ldots \quad \ldots \quad (107)$$

by equations (74) and (102).

91

4.2. *Wings Near Sonic Speed.*—For Mach numbers near unity, β is very small and the plan-form term

$$\frac{2b_a}{a_a c} = \frac{2}{a_a \, . \, c/\bar{c}} A_a = \frac{2}{a_a \, . \, c/\bar{c}} \beta A$$

in the span loading equation (15) of the analogous wing tends to zero*. This demonstrates the close resemblance between wings near sonic speed and wings of small aspect ratio. If the above term, multiplied by γ_a/α_a, can be ignored compared with 1, equation (15) reduces to

$$\frac{\omega_a}{2\pi} \int_{-1}^{+1} \frac{d\left(\frac{\gamma_a}{\alpha_a}\right)}{d\eta'} \frac{d\eta'}{\eta - \eta'} = 1, \quad \text{with} \quad \omega_a \to 2 \quad \ldots \qquad (108)$$

for a flat wing of any plan form. This corresponds exactly to equation (18), and the solution of equation (108) is

$$\frac{\gamma_a}{\alpha_a} = \sqrt{(1 - \eta_a^2)}, \quad \text{or} \quad \frac{\gamma}{\alpha} = \sqrt{(1 - \eta^2)} \quad \ldots \qquad (109)$$

by equation (104). This states that a flat wing has an elliptic span loading near sonic speed, with the overall lift coefficient

$$\frac{\bar{C}_L}{\alpha} = A \int_{-1}^{+1} \sqrt{(1 - \eta^2)} \, d\eta = \frac{\pi}{2} A \quad \ldots \qquad (110)$$

by equations (105) and (107). These are the same results as were obtained by R. T. Jones[2]. A recent, more detailed, investigation of wings at sonic speed by K. W. Mangler[61] has shown that some wing plan forms give less lift than $\pi A/2$, owing to the effect of a system of incipient shock-waves occurring at sonic speed. In reality, shock-waves caused by the thickness of the wing will usually occur below sonic speed; these, and boundary-layer effects, will invalidate any method based on a linearised theory for thin wings at small lift in inviscid flow, and the theoretical lift will not be obtained. The calculation method can thus be applied only for Mach numbers below the critical.

4.3. *Approximate Rules for Estimation Purposes.*—To obtain an estimate for the variation of the overall lift coefficient with Mach number, we may use Helmbold's formula for elliptic span loading in its extended form, equation (81). With equations (101) and (102), we find

$$\frac{\bar{C}_L}{\alpha} = \frac{a_0 \cos\varphi}{\sqrt{\left\{1 - M_0^2 \cos^2\varphi + \left(\frac{a_0 \cos\varphi}{\pi A}\right)^2\right\}} + \frac{a_0 \cos\varphi}{\pi A}} \quad \ldots \qquad (111)$$

This relation was first derived in a different way by H. Ludwieg[30] for straight wings. Equation (111) includes the special case of the sheared wing of infinite aspect ratio, where

$$\frac{\bar{C}_L}{\alpha} = \frac{a_0 \cos\varphi}{\sqrt{(1 - M_0^2 \cos^2\varphi)}}, \quad \ldots \qquad (112)$$

which also follows from equation (78) with $n_{sa} = \frac{1}{2}$, which gives $C_{La}/\alpha_a = a_0 \cos\varphi_a$; and from equations (100) and (102). Equation (112) is the well-known Prandtl-Glauert rule, which therefore applies only to wings of infinite aspect ratio. Equation (111) does not give the correct limit for $M_0 \to 1$:

$$\frac{\bar{C}_L}{\alpha} = \frac{\pi A}{2} \frac{2}{1 + \sqrt{(1 + \frac{1}{4}A^2 \tan^2\varphi)}}, \quad \ldots \qquad (113)$$

which is equal to $\pi A/2$ only for $\varphi = 0$.

* a_a tends to zero like $\sqrt{(\beta A)}$, by equation (83), since the effective sweep of the analogous wing $\varphi_{ea} \to 0$ as $A_a = \beta A \to 0$, by equation (86).

As an illustration, Fig. 30 shows measured and calculated overall lift values at various Mach numbers. It can be seen that neither equation (111) nor equation (112) gives a sufficiently accurate estimate in these cases. It appears that equation (iii) gives a reasonable estimate only for wings of small aspect ratio, in particular for straight wings, as shown in Ref. 30. For the wings in Fig. 30, good agreement is obtained only when the spanwise load distribution is calculated first from the present method and the overall lift coefficient obtained afterwards by integration (full lines). It may happen in such a calculation that the lift at $M_0 < 1$ is greater than the limit as $M_0 \to 1$, equation (110), so that this limit is approached from above. This development is usually cut short, however, by the occurrence of shock-waves before $M_0 = 1$ is reached. In the special cases of Fig. 30, such shock-waves occur before the steeper lift rise begins and the measured lift drops near $M_0 = 0 \cdot 9$.

These examples indicate that ' rules ' like equation (111) or (112) may give misleading results. The need for such rules, however, hardly exists any longer since the present method enables the full aerodynamic properties of a given wing at a given Mach number to be quickly and reliably estimated.

REFERENCES

No.	Author	Title, etc.
1	L. Prandtl	Tragflügeltheorie. I. Mitteilung. Nachrichten der Königlichen Gesellschaft der Wissenschaften zu Göttingen. Math. Phys. Klasse, p. 451. 1918.
2	R. T. Jones	Properties of low-aspect-ratio pointed wings at speeds below and above the speed of sound. N.A.C.A. Report 835. 1946.
3	D. Küchemann	The distribution of lift over the surface of swept wings. *Aero. Quart.*, Vol. IV, p. 261. August, 1953.
4	G. G. Brebner	The application of camber and twist to swept wings in incompressible flow. C.P. 171. March, 1952.
5	G. G. Brebner	The calculation of the loading and pressure distribution on cranked wings. R.A.E. Report Aero. 2483. A.R.C. 15,933. January, 1953.
6	J. Weber, D. A. Kirby and D. J. Kettle ..	An extension of Multhopp's method of calculating the spanwise loading of wing-fuselage combinations. R. & M. 2872. November, 1951.
7	D. E. Hartley	Theoretical load distributions on wings with cylindrical bodies at the tips. C.P. 147. June, 1952.
8	J. Weber	Theoretical load distributions on a wing with a cylindrical body at one end. R. & M. 2889. June, 1952.
9	B. A. Hunn	A method of estimating the loading on an elastic airframe. *J. R. Ae. Soc.*, Vol. 56, p. 261. April, 1952.
10	J. Weber	The calculation of the pressure distribution over the surface of two-dimensional and swept wings with symmetrical aerofoil sections. R. & M. 2918. July, 1953.
11	G. G. Brebner and J. A. Bagley ..	Boundary-layer and pressure measurements on a two-dimensional wing at low speed. R. & M. 2886. February, 1952.
12	W. Birnbaum	Die tragende Wirbelfläche als Hilfsmittel zur Behandlung des ebenen Problems der Tragflügeltheorie. *Z.A.M.M.*, Vol. 3, p. 290. 1923.
13	D. Küchemann	Some methods of determining the effect of the boundary layer on the lift slope of straight and swept wings. R.A.E. Tech. Note Aero. 2167. A.R.C. 15245. 1952. (Unpublished.)

14 D. Küchemann .. .. Bemerkung über den Einfluss des Seitenverhältnisses auf den Zusammenhang von Normalkraft und Tangentialkraft eines Tragflügels. *Z.A.M.M.*, Vol. 20, p. 290. 1940; and Vol. 22, p. 304. 1942.

15 L. Prandtl and A. Betz .. .. Experimentelle Prüfung der Umrechnungsformeln. Ergebnisse der AVA Göttingen, I. Lieferung, p. 50. 1920.

16 H. R. Lawrence .. .. The lift distribution on low aspect ratio wings at subsonic speeds. *J. Ae. Sci.*, Vol. 18, p. 683. 1951.

17 H. Multhopp .. .. Die Berechnung der Auftriebsverteilung von Tragflügeln. *L.F.F.*, Vol. 15, p. 153. 1938. Translation: A.R.C. 8516.

18 C. H. Zimmerman .. .. .. Characteristics of Clark Y airfoils of small aspect ratio. N.A.C.A. Report 431. 1932.

19 N. Scholz .. .. Beiträge zur Theorie der tragenden Fläche. *Ing. Arch.*, Vol. 18, p. 84. 1950; and Kraft- und Druckverteilungsmessungen and Tragflächen kleiner Streckung. *Forschung.*, Vol. 16, p. 85. 1949/50.

20 H. Voepel (edited F. N. Kirk) .. .. Tests on wings of small aspect ratio. R.A.E. Library Trans. No. 276. A.R.C. 12,450. 1948.

21 J. Weissinger .. .. Über die Auftriebsverteilung von Pfeilflügeln. Forschungsbericht FB 1533. 1942. Translation: N.A.C.A. Tech. Memo No. 1120.

22 J. De Young and C. W. Harper .. Theoretical symmetric span loading at subsonic speeds for wings having arbitrary planform. N.A.C.A. Report 921. 1948.

23 V. M. Falkner .. .. The calculation of aerodynamic loading on surfaces of any shape. R. & M. 1910. 1943.

The solution of lifting plane problems by vortex lattice theory. R. & M. 2591. September, 1947.

24 W. Kinner.. .. .. Die kreisförmige Tragfläche auf potentialtheoretischer Grundlage. *Ing. Archiv.*, Vol. 8, p. 47. 1937. TIB Trans. No. 2345.

25 K. Krienes .. .. Die elliptische Tragfläche auf potentialtheoretischer Grundlage. *Z.A.M.M.*, Vol. 20, p. 65. 1940.

26 K. Wieghardt .. .. Über die Auftriebsverteilung des einfachen Rechteckflügels über die Tiefe. *Z.A.M.M.*, Vol. 19, p. 257. 1939. Trans.: N.A.C.A. Tech. Memo. 963.

27 H. Multhopp .. .. Methods for calculating the lift distribution of wings (subsonic lifting-surface theory). R. & M. 2884. January, 1950.

28 E. Pistolesi .. .. Considerazioni sul problema del biplano. *Aerotecnica.*, Vol. 13, p. 185. 1933.

29 H. B. Helmbold .. .. Der unverwundene Ellipsenflügel als tragende Fläche. *Jahrb.* 1942 *d. deutschen Luftfahrtforschung.*

30 H. Ludwieg .. .. Aerofoil theory in the compressible region. AVA Monograph $F_1$4. Ministry of Supply R. & T. 1026. 1948.

31 F. W. Diederich .. .. A plan-form parameter for correlating certain aerodynamic characteristics of swept wings. N.A.C.A. Tech. Note 2335. 1951.

32 L. Prandtl and O. Tietjens .. .. Hydro- und Aeromechanik, Vol. ii, p. 202. Translation: McGraw-Hill Book Company, New York.

33 M. M. Munk .. .. Isoperimetrische Aufgaben aus der Theorie des Fluges. Dissertation Göttingen. 1919.

34 G. N. Ward .. .. Supersonic flow past slender pointed bodies. *Q. J. Mech. App. Math.*, Vol. 2, p. 75. 1949.

REFERENCES—*continued*

35 W. Bollay .. .. A non-linear wing theory and its application to rectangular wings of small aspect ratio. *Z.A.M.M.*, Vol. 19, p. 21. 1939.

36 F. Weinig .. .. Beitrag zur Theorie des Tragflügels endlicher insbesondere kleiner Spannweite. *L.F.F.*, Vol. 13, p. 405. 1936. Translation: N.A.C.A. Tech. Memo. 1151.

37 A. H. Flax and H. R. Lawrence .. The aerodynamics of low-aspect-ratio wings and wing-body combinations. Third Int. Conf., Brighton, 1951.

38 W. Mangler .. .. Der kleinste induzierte Widerstand eines Tragflügels mit kleinem Seitenverhältnis. *Jahrb.* 1939 *d. deutschen Luftfahrtforschung*, p. I, 140.

39 W. Mangler .. .. Die Auftriebsverteilung am Tragflügel mit seitlichen Scheiben. *L.F.F.*, Vol. 16, p. 219. 1939. Translation: TIB 2338.

40 W. Mangler and J. Rotta .. .. Aerofoils with tip plates. AVA Monogragh $F_1$6. Ministry of Supply, R. & T. 1023. 1947.

41 D. Küchemann and D. J. Kettle .. The effect of endplates on swept wings. C.P. 104. June, 1951.

42 J. Weber .. .. Low speed measurements of the pressure distribution near the tips of swept wings at no lift. R.A.E. Report Aero. 2318. A.R.C. 12,421. 1949.

43 F. B. Bradfield .. .. Centre of pressure travel of symmetrical sections at small incidence. R.A.E. Report B.A. 840. 1929.

44 D. Küchemann and J. Weber .. On the chordwise lift distribution at the centre of swept wings *Aero. Quart.*, Vol. 2, p. 146. 1950.

45 H. C. Garner .. .. .. Swept-wing loading. A critical comparison of four subsonic vortex sheet theories. C.P. 102. July, 1951.

46 J. Weber and G. G. Brebner .. .. Low-speed tests on 45-deg swept-back wings. Part I: Pressure measurements on wings of aspect ratio 5. R. & M. 2882. May, 1951.

47 D. Küchemann and J. Weber .. .. The subsonic flow past swept wings at zero lift without and with body. R. & M. 2908. March, 1953.

48 W. S. D. Marshall .. .. .. The distribution of pressure over the surface of wings of small aspect ratio. College of Aeronautics, Report No. 52. A.R.C. 14937. 1952.

49 C. E. Brown .. .. The reversibility theorem for thin airfoils in subsonic and supersonic flow. N.A.C.A. Report 1944. 1949.

50 M. M. Munk .. .. The reversal theorem of linearised superonic airfoil theory. *J. App. Phys.*, Vol. 21, p. 159. 1950.

51 D. Küchemann, J. Weber and G. G. Brebner Low-speed tests on wings of 45-deg sweep. Part II: Balance and pressure measurements on wings of different aspect ratios. R. & M. 2882. May, 1951.

52 R. Stanton Jones .. .. .. An empirical method for rapidly determining the loading distributions on swept-back wings. College of Aeronautics Report No. 32. A.R.C. 12,997. January, 1950.

53 H. C. Garner .. .. Theoretical calculations of the distribution of aerodynamic loading on a delta wing. R. & M. 2819. March, 1949.

54 K. Orlik - H. Rückemann .. .. Experimental determination of pressure distributions and transition lines of plane delta wings at low speeds and zero yaw. Swedish Tech. Note KTH–Aero No. 3. 1949.

55 J. H. Preston .. .. The calculation of lift taking account of the boundary layer. R. & M. 2725. November, 1949.

56 J. Weber .. .. Low-speed measurements of the pressure distributions and overall forces on wings of small aspect ratio and 53-deg sweepback. R.A.E. Tech. Note Aero. 2017. A.R.C. 12,878. 1949. (Unpublished.)

57	A. Busemann	Profilmessungen bei Geschwindigkeiten nahe der Schallgeschwindigkeit. *Jahrb. d. wiss. Gesellschaft für Luftfahrt.* 1928.
58	B. Göthert	Ebene und räunliche Strömung bei hohen Unterschallgeschwindigkeiten. *Jahrb. d. deutschen Luftfahrtforschung,* I p. 135. 1941.
59	Th. von Kármán	Compressibility effects in aerodynamics. *J. Ae. Sci.,* Vol. 8, p. 337. 1941.
60	J. Weber	Application of the theory of incompressible flow around a swept wing at zero incidence to the flow at high subsonic Mach numbers. R.A.E. Report Aero. 2274. A.R.C. 11,774. 1948.
61	K. W. Mangler	Calculation of the pressure distribution over a wing at sonic speeds. R. & M. 2888. September, 1951.
62	B. E. Tinling and W. R. Kolk	The effects of Mach number and Reynolds number on the aerodynamic characteristics of several 12-per-cent-thick wings having 35 deg of sweepback and various amounts of camber. N.A.C.A. Research Memo. A50K27. TIB/2629. 1951.

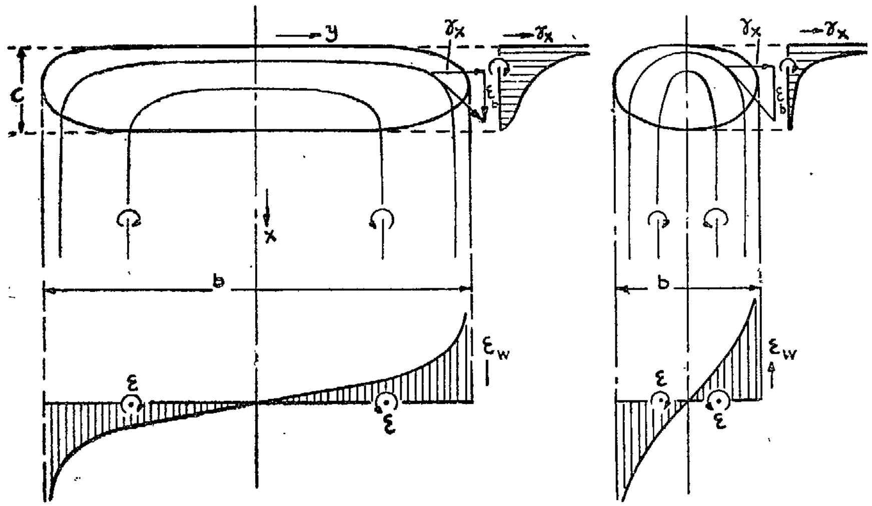

FIG. 1. Vortex system on wings.

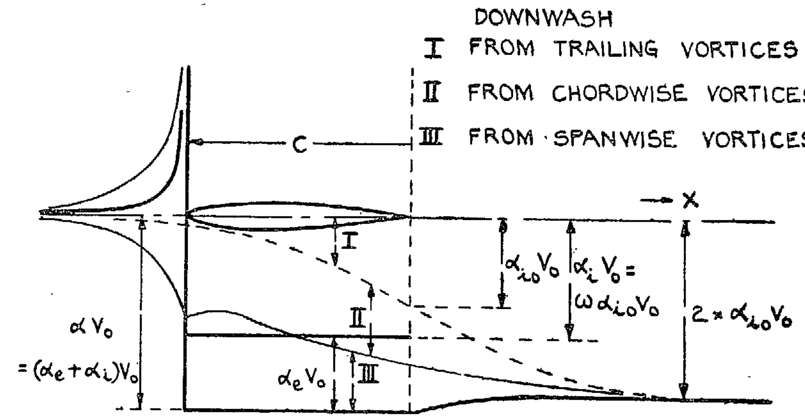

FIG. 3. Streamwise downwash distributions.

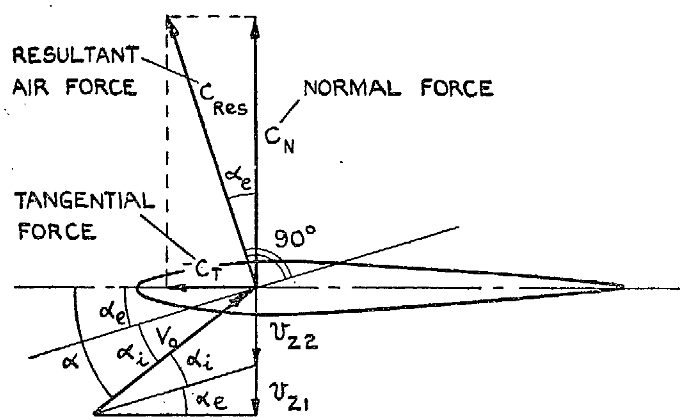

FIG. 2. Definition of forces and angles.

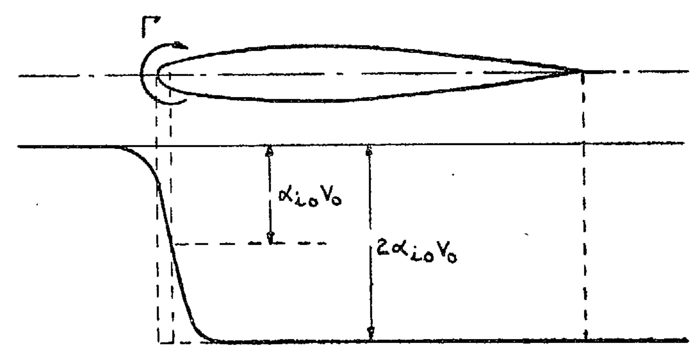

FIG. 4. Downwash on aerofoil of very small aspect ratio.

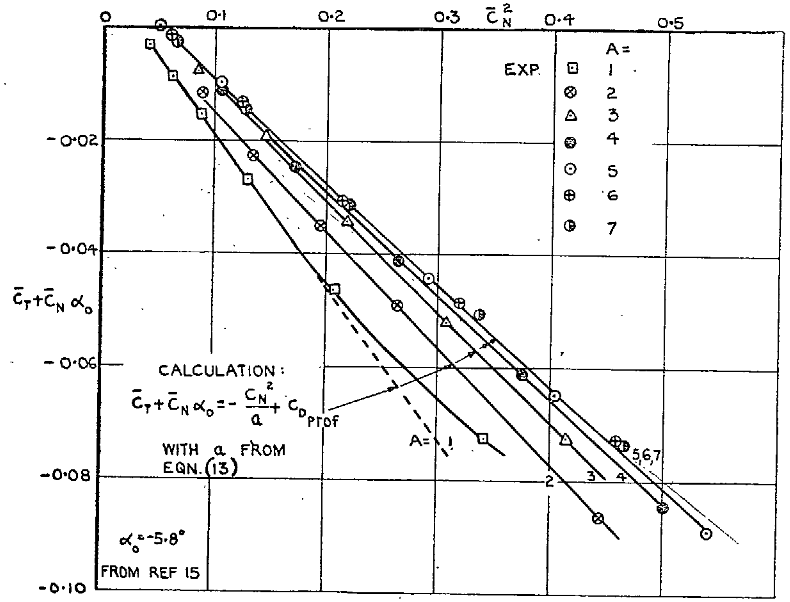

FIG. 5.

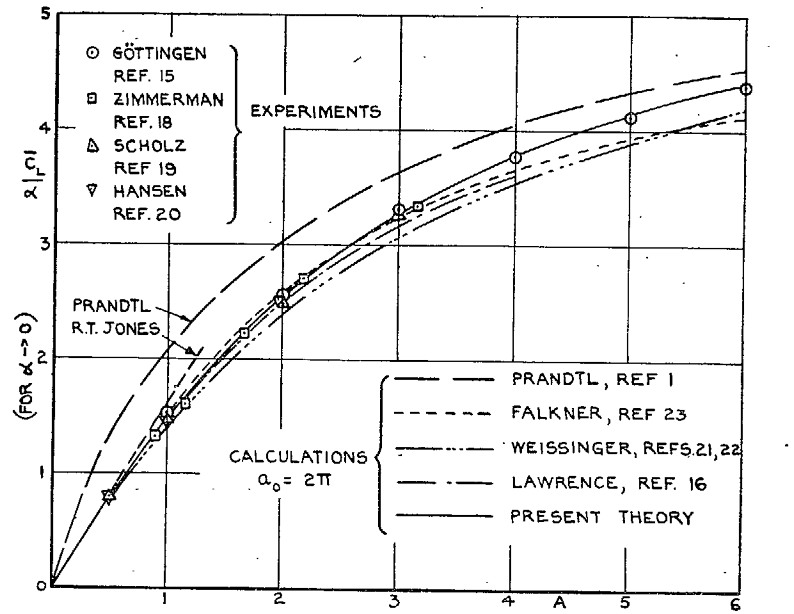

FIG. 6.

FIGS. 5 and 6. Forces on straight wings of constant chord.

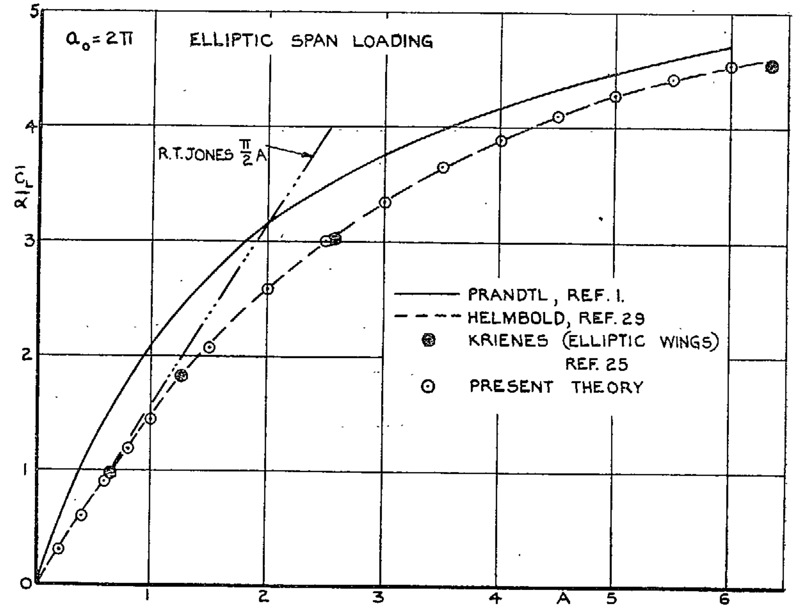

FIG. 7.

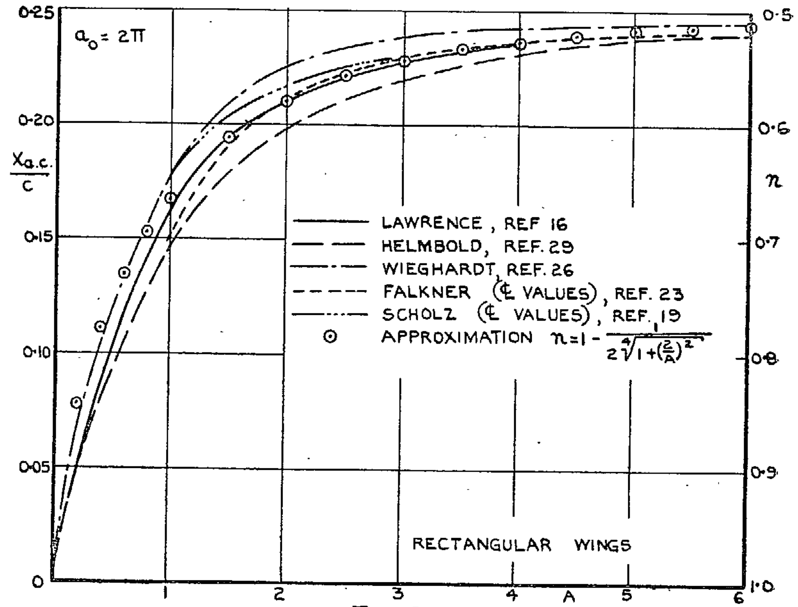

FIG. 8.

FIGS. 7 and 8. Overall lift and aerodynamic centre position of straight wings.

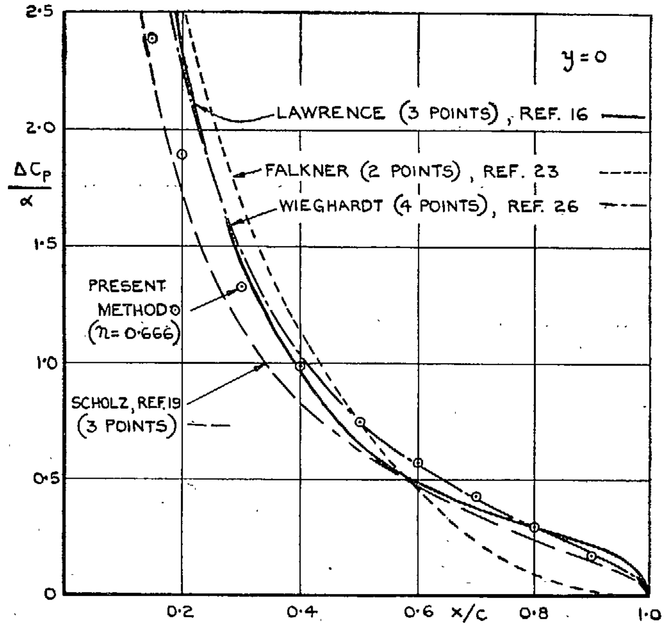

Fig. 9.

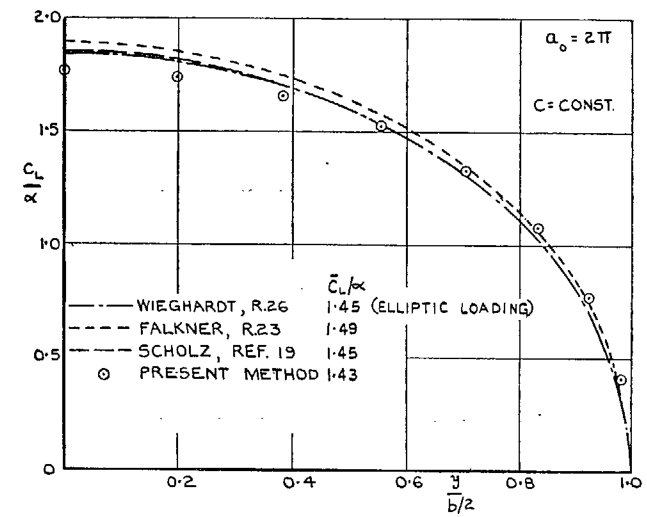

Fig. 10.

Figs. 9 and 10. Chordwise and spanwise loading on square wing ($A = 1$).

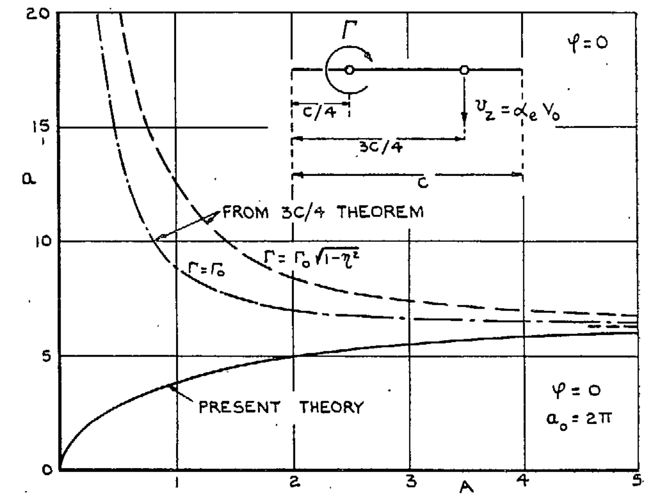

Fig. 11.

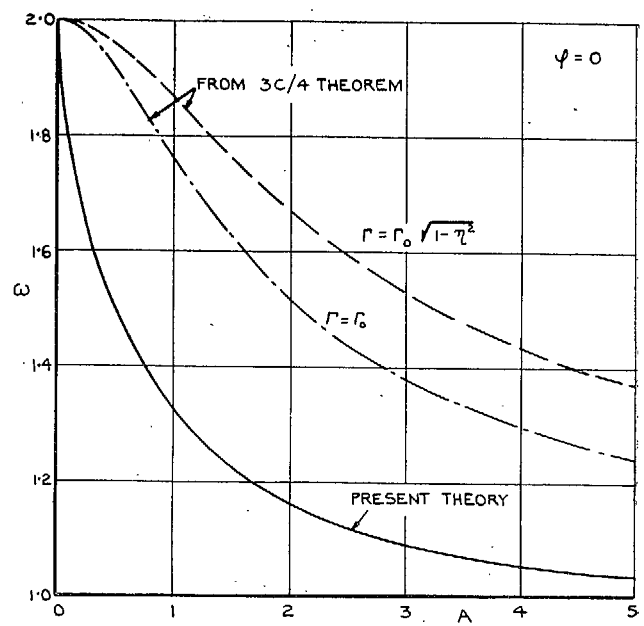

Fig. 12.

Figs. 11 and 12. Sectional lift slope and downwash factor from three-quarter chord theorem.

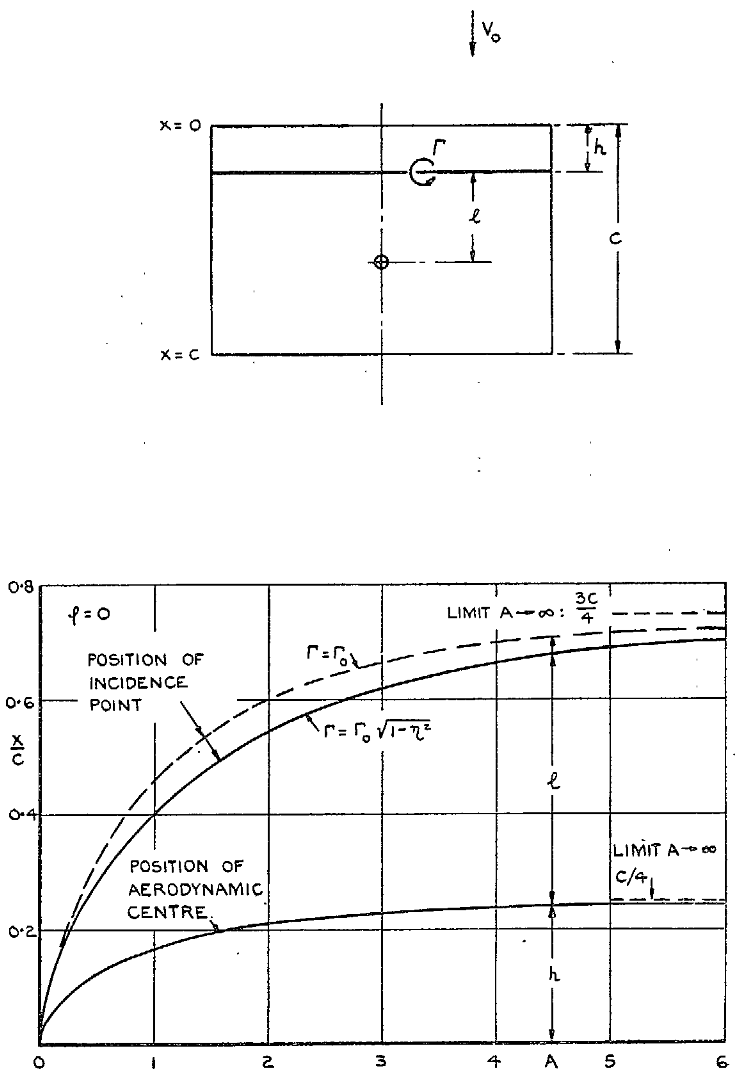

FIG. 13. Variation of 'incidence point' with aspect ratio.

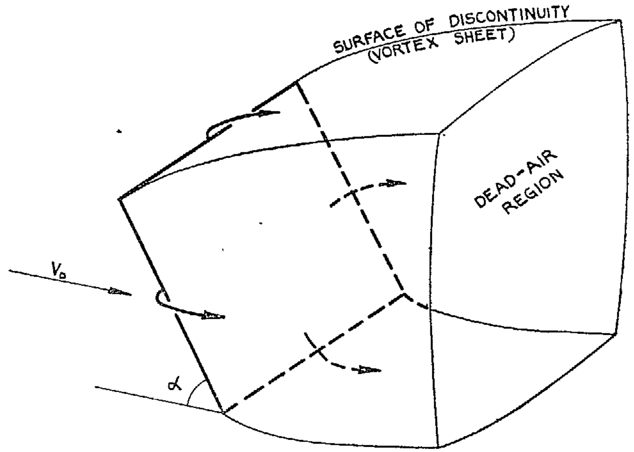

FIG. 14a. α Large ($\alpha > \alpha_{max}$). Flow separation at all four edges.

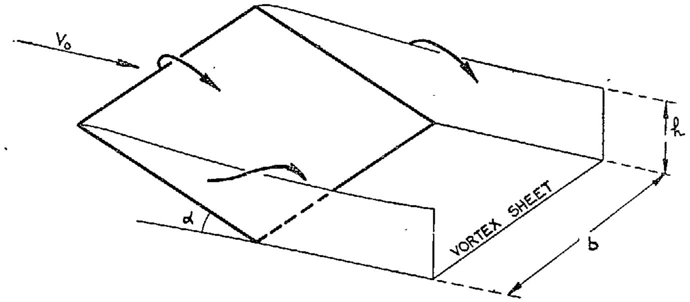

FIG. 14b. α moderate ($\alpha > \alpha_S$). Flow attached at leading edge.

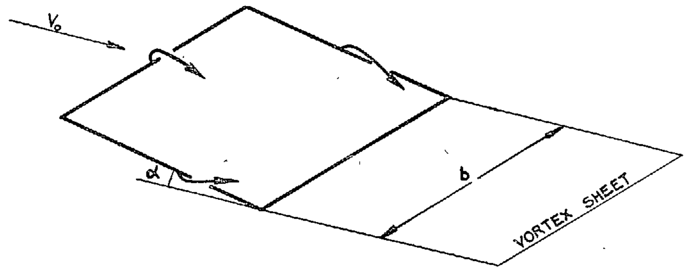

FIG. 14c. α Small ($\alpha > \alpha_S$). Flow attached at leading edge and sides.

FIGS. 14a, 14b and 14c. Sketch of possible flow patterns.

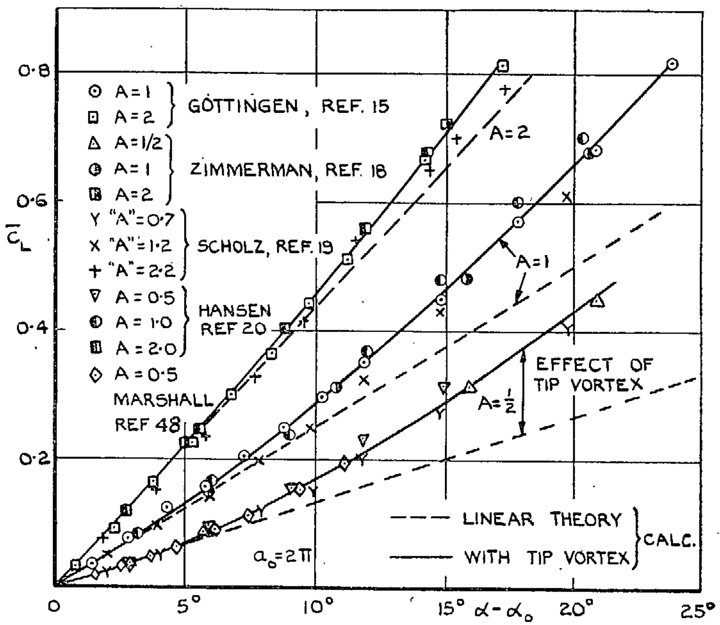

FIG. 15. Overall lift of rectangular wings.

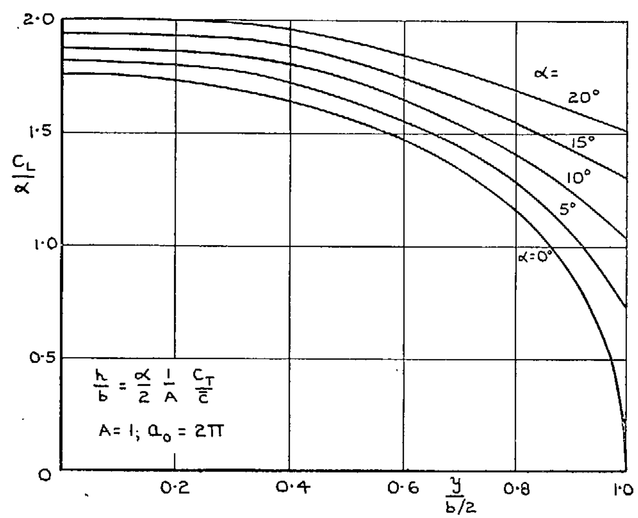

FIG. 16. Spanwise loadings on a square wing (calculated).

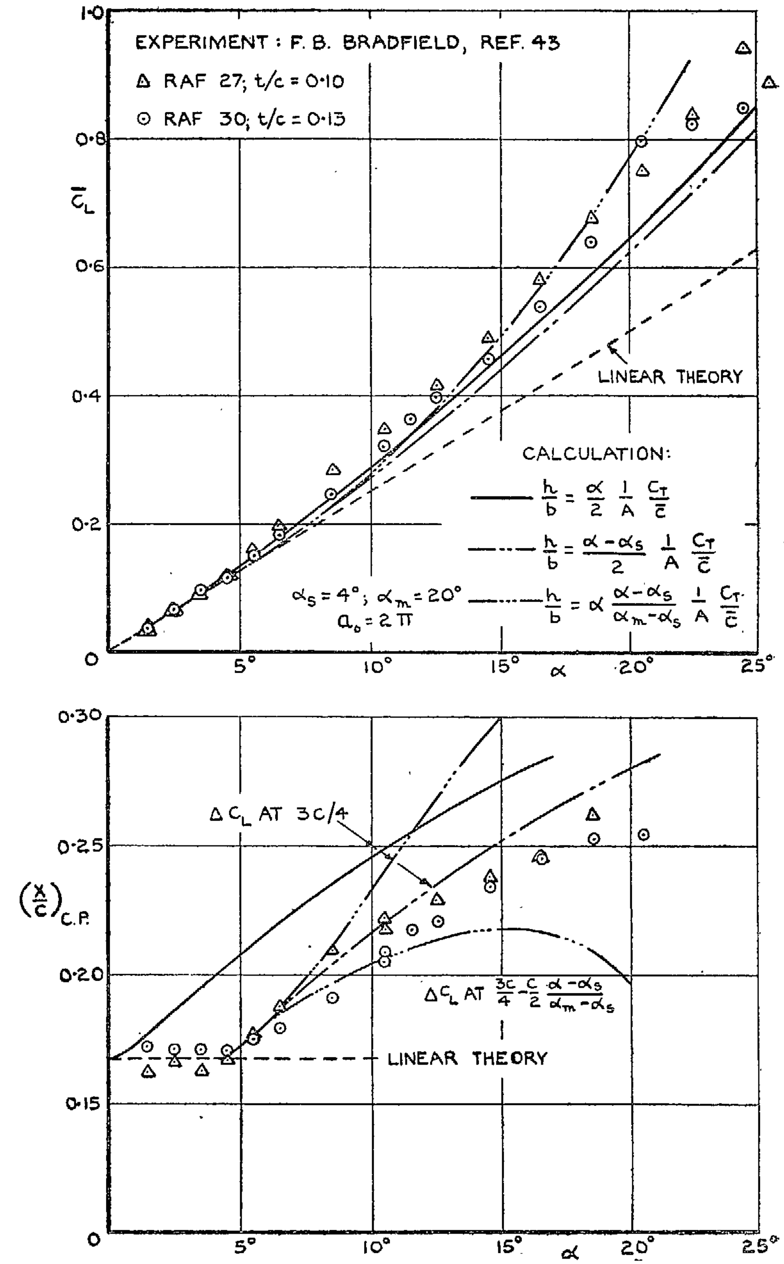

FIG. 17. Overall lift and position of c.p. on square wings. From Ref. 43.

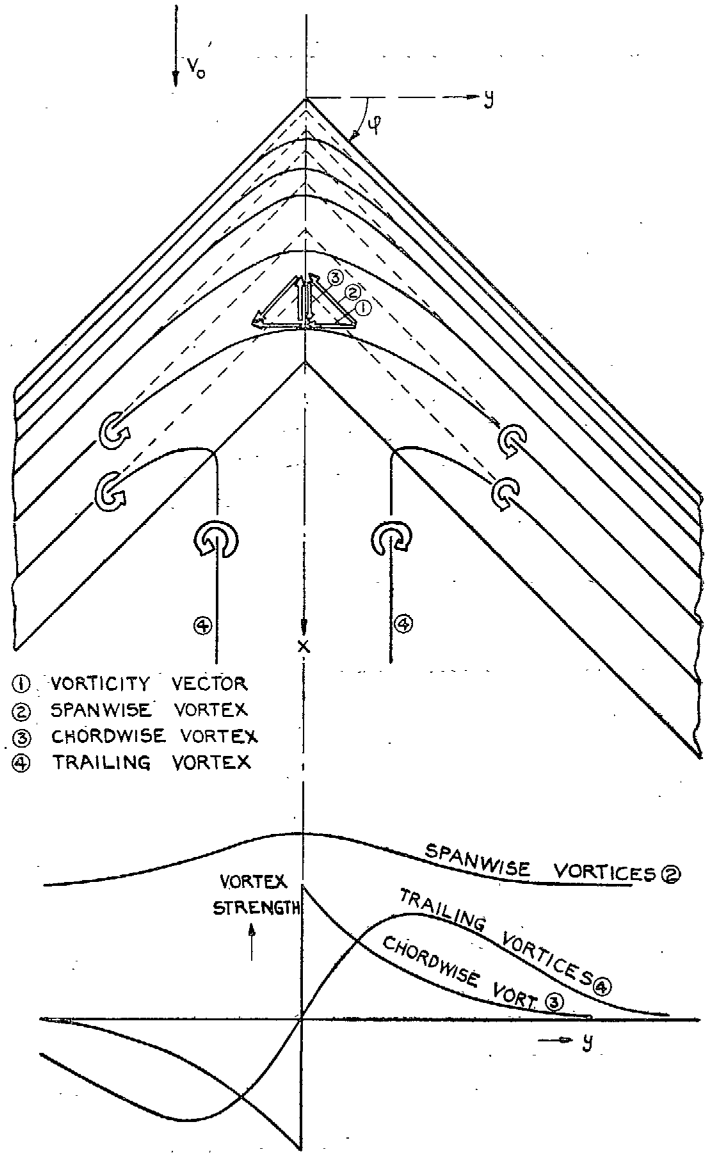

FIG. 18. Vortex system near the centre of a swept wing (schematic).

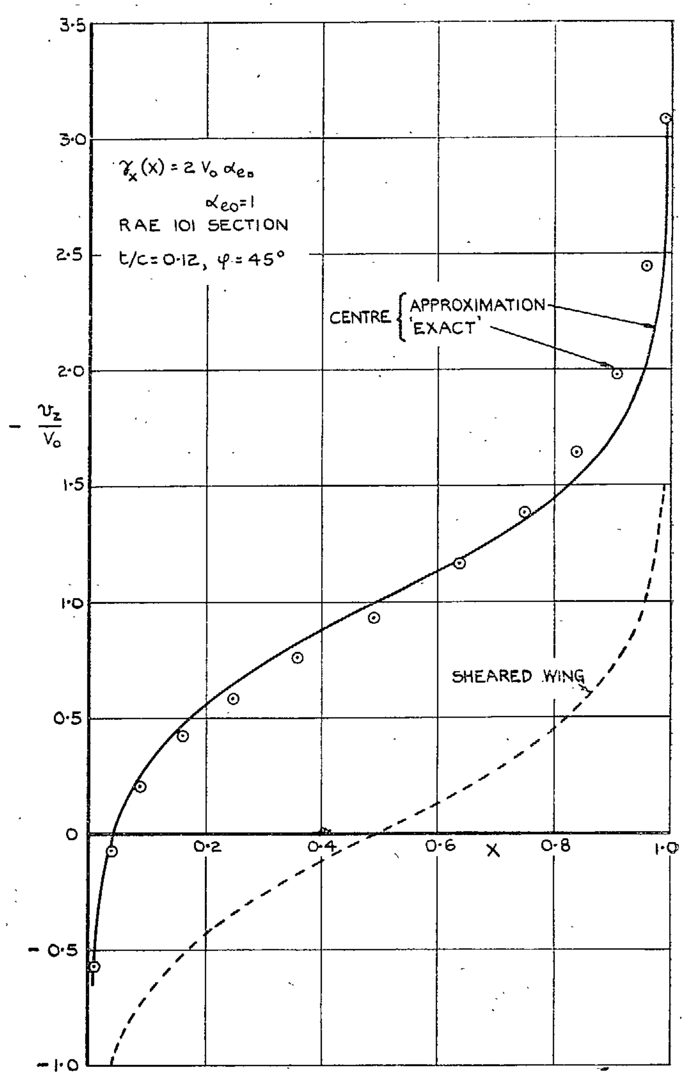

FIG. 19. Calculated downwash on a swept wing with uniform span- and chord-wise loading.

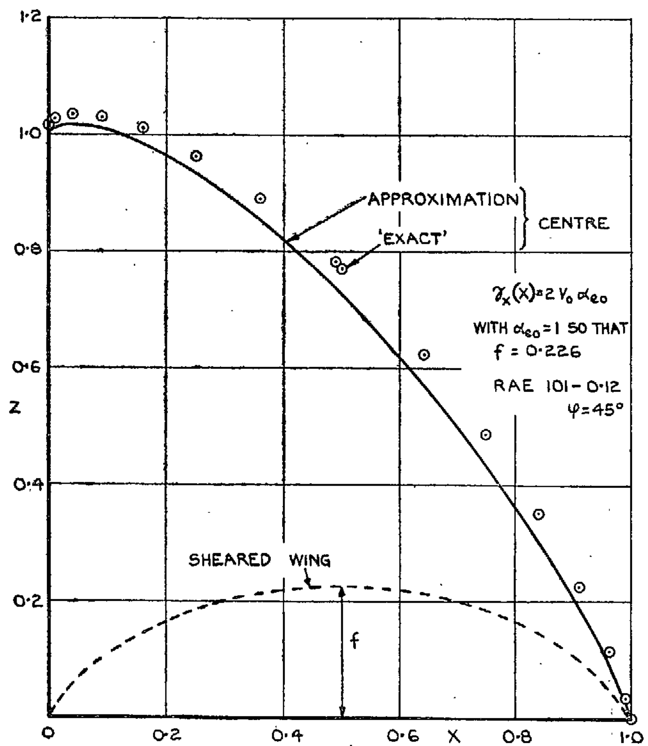

FIG. 20. Calculated chord-line shapes for a swept wing with uniform span- and chord-wise loading.

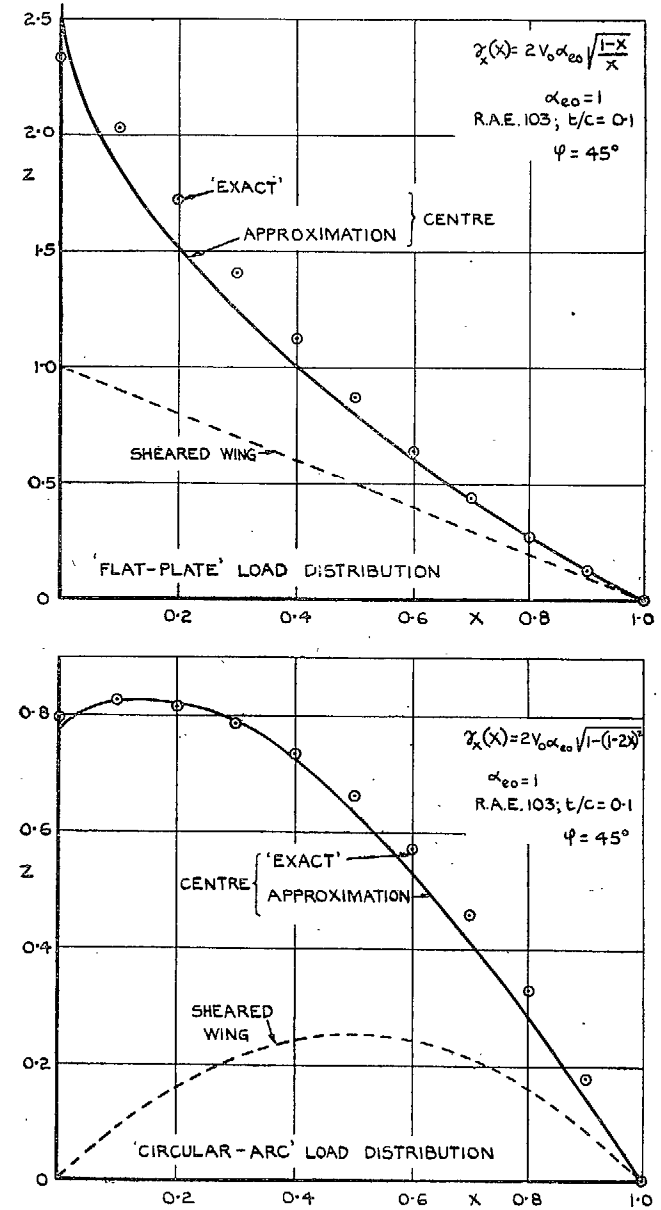

FIG. 21. Calculated chord-line shapes for swept wings with uniform span loading, but different chordwise loadings.

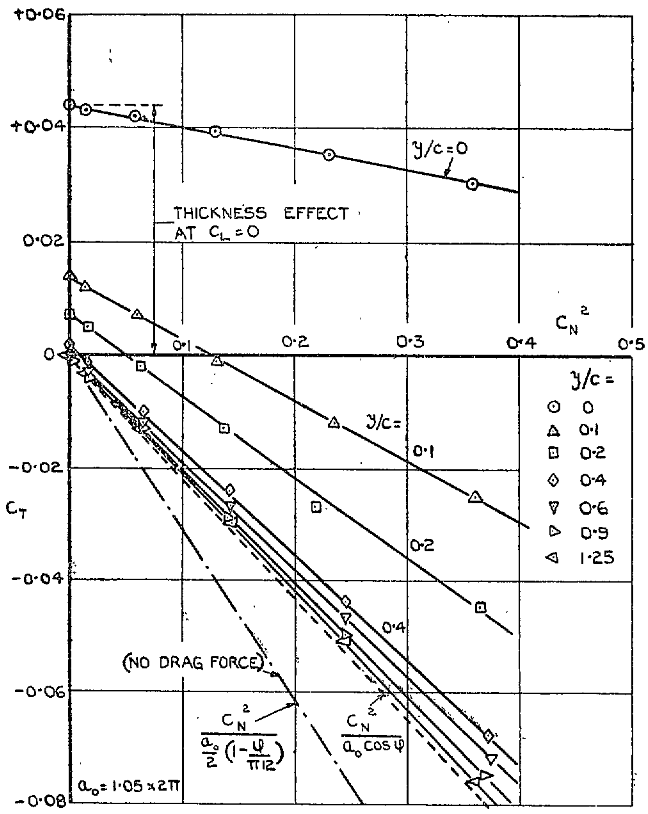

FIG. 22. Measured normal and tangential force coefficients at various spanwise stations of a 45-deg swept-back constant-chord wing of aspect ratio 5. From Ref. 46.

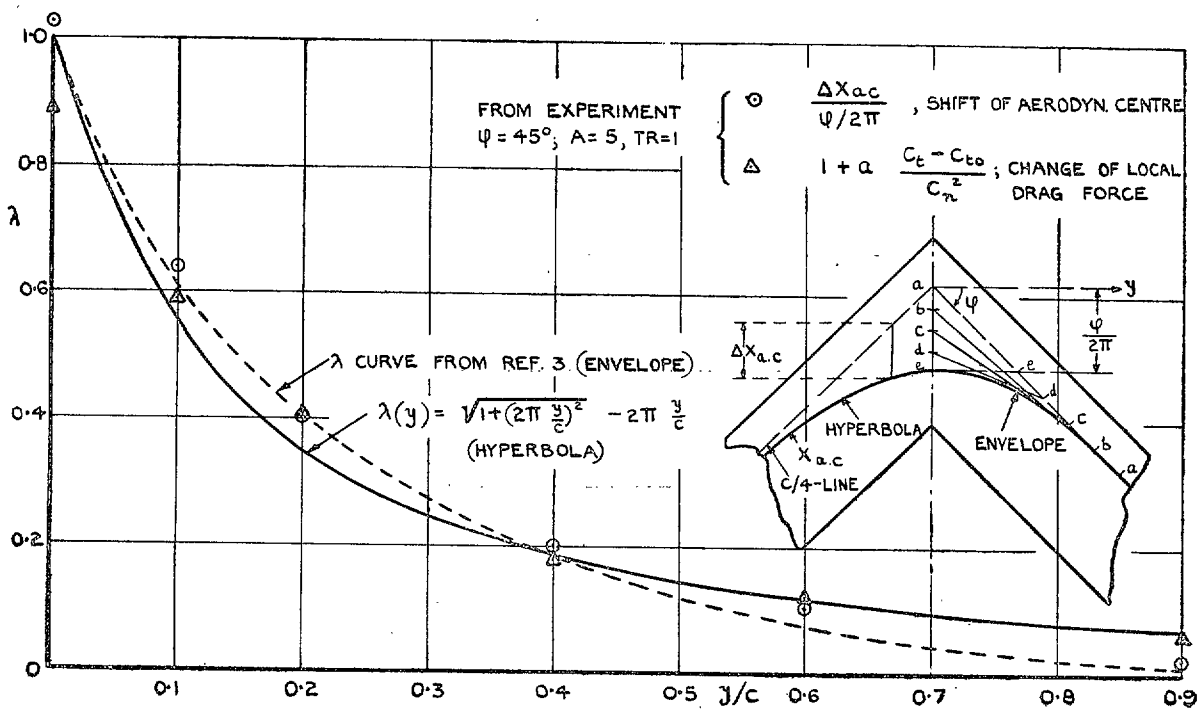

FIG. 23. Interpolation curve $\lambda(y)$.

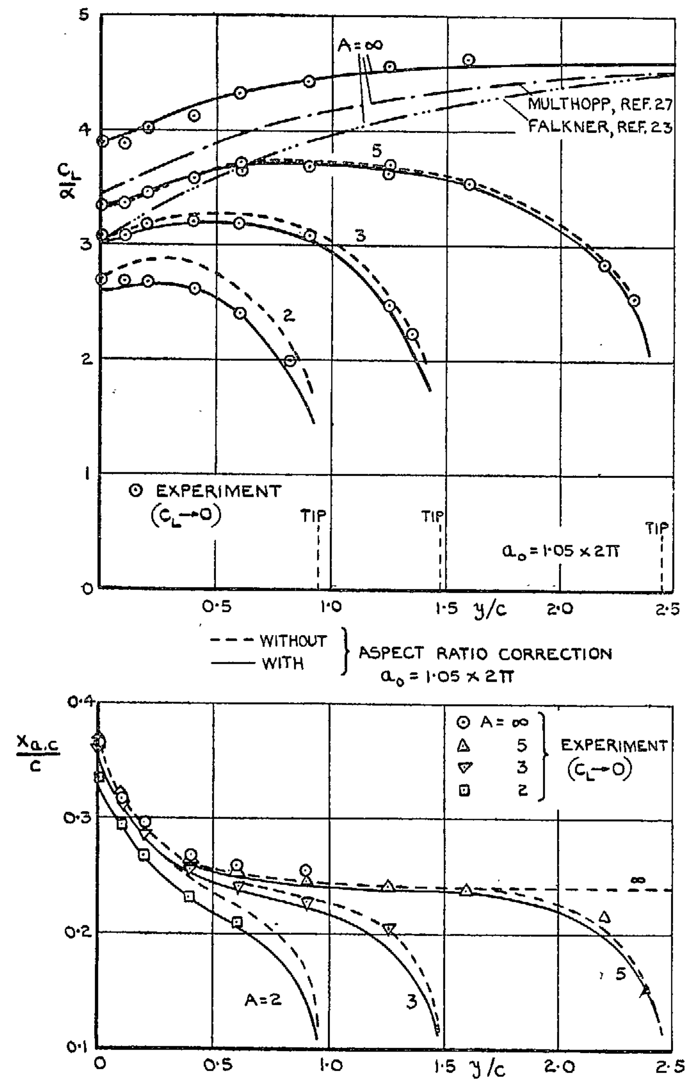

FIG. 24. Measured and calculated spanwise lift distribution and aerodynamic centre positions on 45-deg sweptback wings of constant chord. From Refs. 46 and 51.

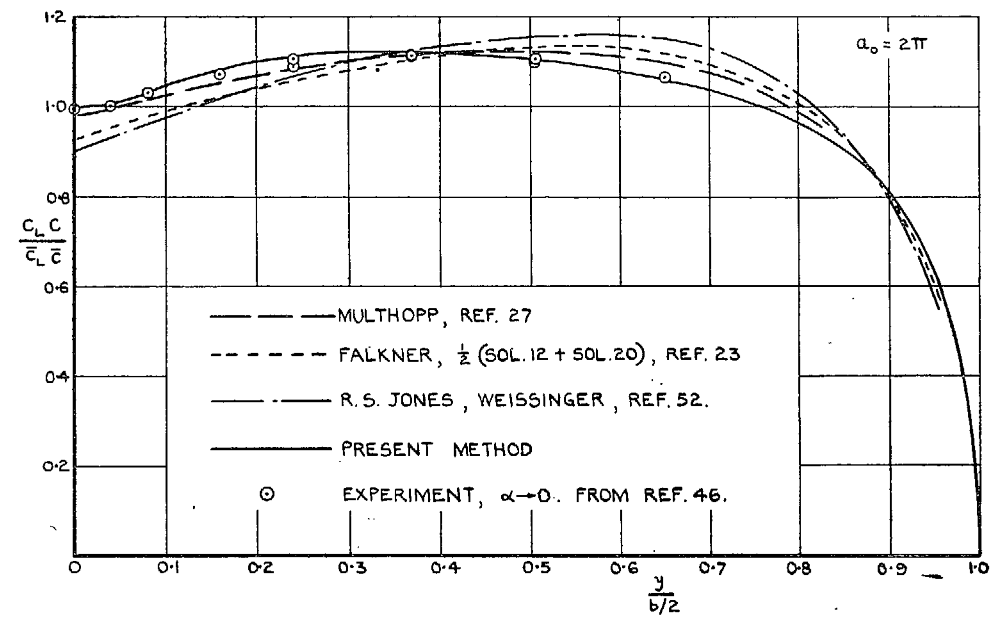

FIG. 25. Span loadings for a 45-deg swept-back constant-chord wing. $A = 5$.

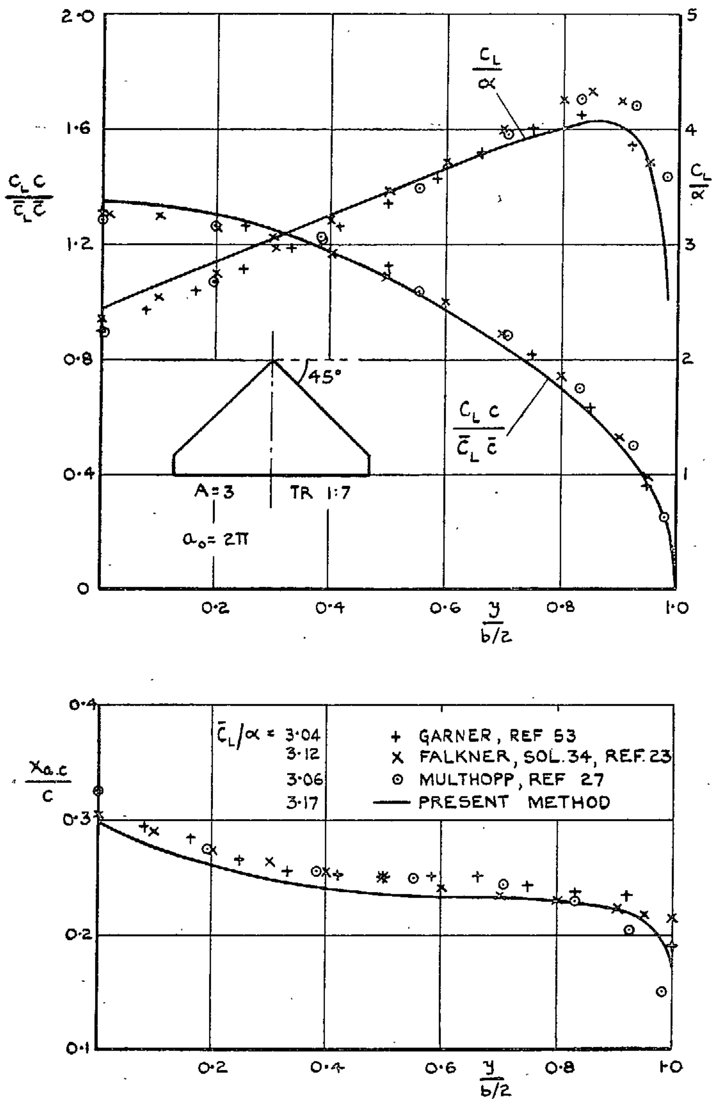

FIG. 26. Calculated span loadings and aerodynamic centre positions for a cropped delta wing.

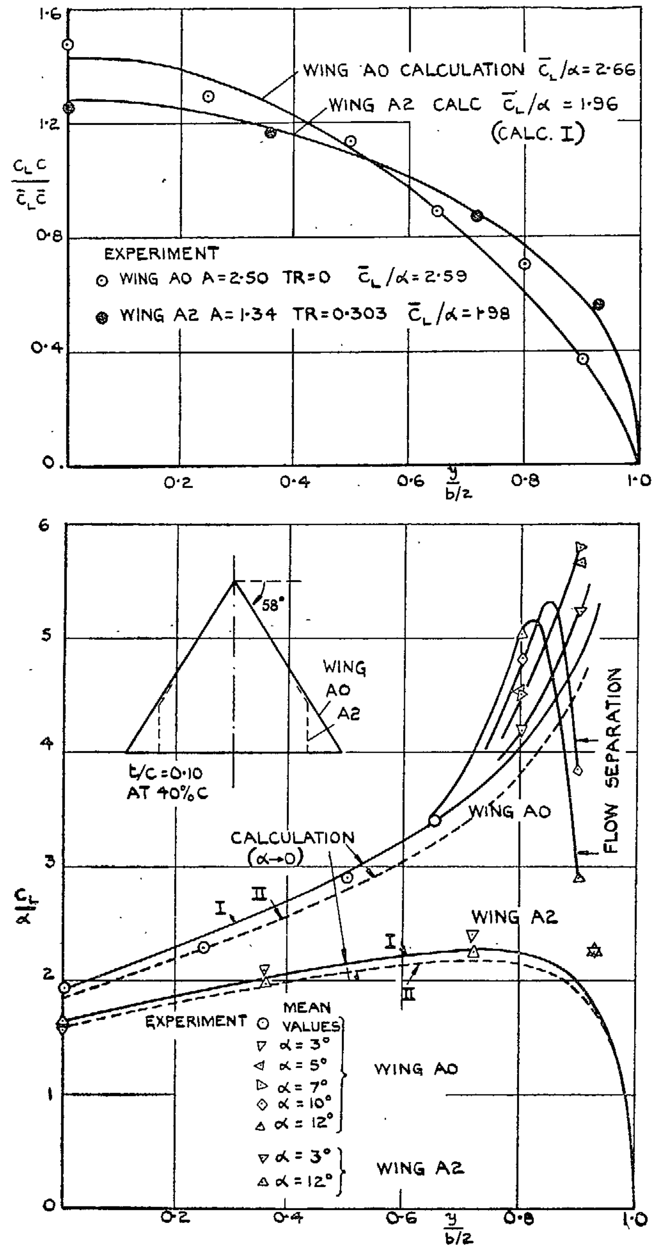

FIG. 27. Measured and calculated span loadings from Ref. 54.

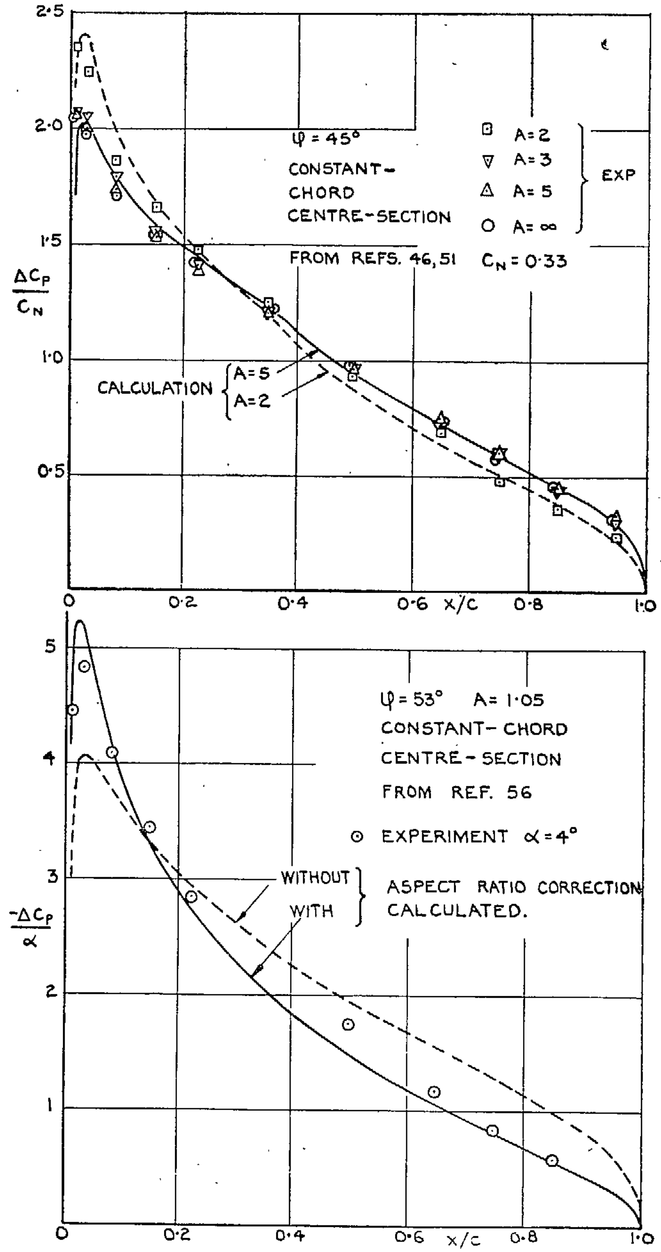

FIG. 28. Measured and calculated chordwise loadings.

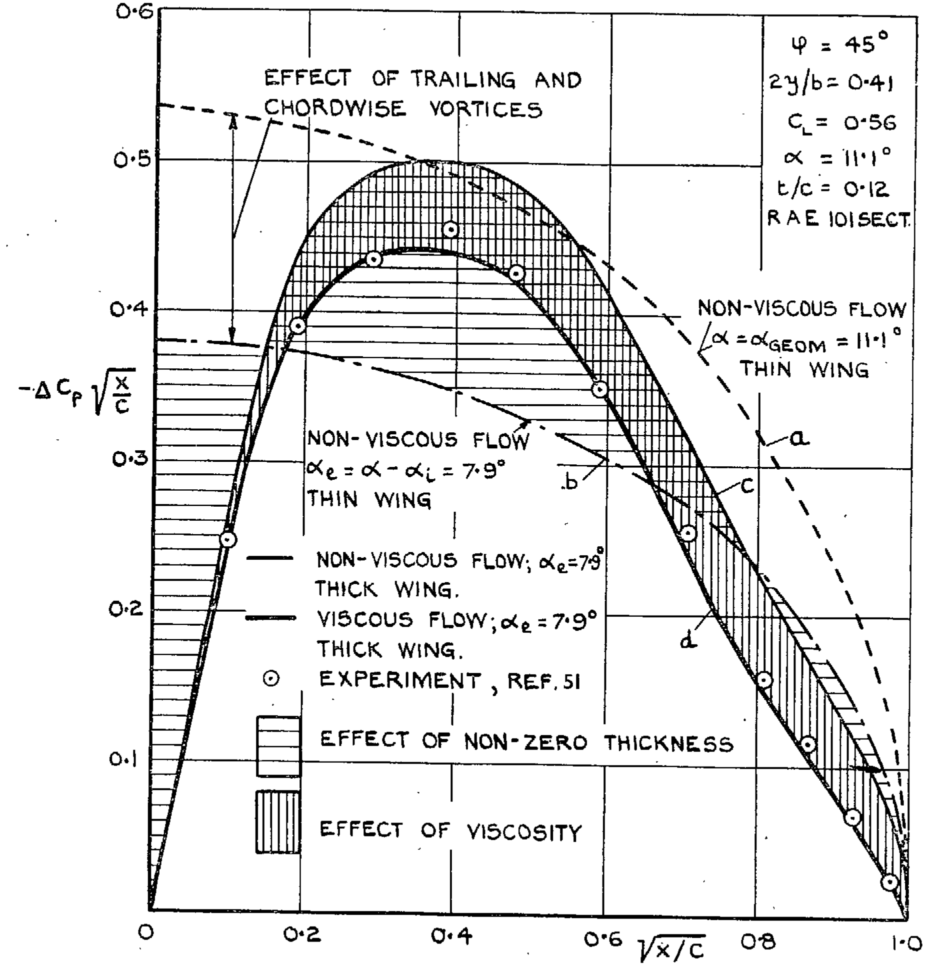

FIG. 29. Chordwise load distribution at about mid-semispan on a 45-deg swept-back constant-chord wing of aspect ratio 3.

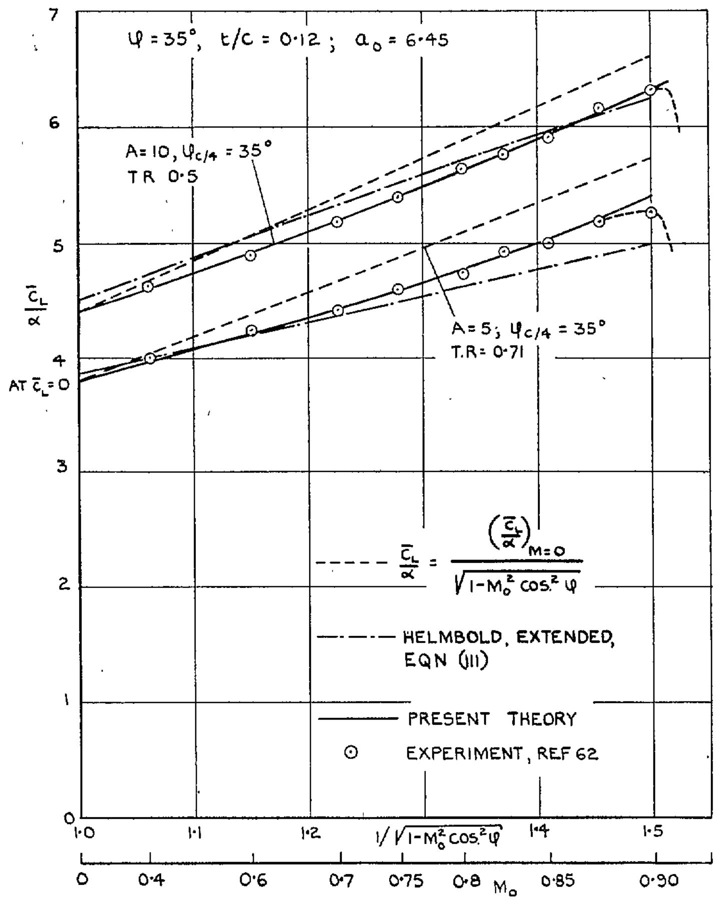

FIG. 30. Measured and calculated variation of overall lift slope with Mach number.

Publications of the Aeronautical Research Council

ANNUAL TECHNICAL REPORTS OF THE AERONAUTICAL RESEARCH COUNCIL (BOUND VOLUMES)

1938 Vol. I. Aerodynamics General, Performance, Airscrews. 50*s.* (51*s.* 8*d.*)
Vol. II. Stability and Control, Flutter, Structures, Seaplanes, Wind Tunnels, Materials. 30*s.* (31*s.* 8*d.*)

1939 Vol. I. Aerodynamics General, Performance, Airscrews, Engines. 50*s.* (51*s.* 8*d.*)
Vol. II. Stability and Control, Flutter and Vibration, Instruments, Structures, Seaplanes, etc. 63*s.* (64*s.* 8*d.*)

1940 Aero and Hydrodynamics, Aerofoils, Airscrews, Engines, Flutter, Icing, Stability and Control, Structures, and a miscellaneous section. 50*s.* (51*s.* 8*d.*)

1941 Aero and Hydrodynamics, Aerofoils, Airscrews, Engines, Flutter, Stability and Control, Structures. 63*s.* (64*s.* 8*d.*)

1942 Vol. I. Aero and Hydrodynamics, Aerofoils, Airscrews, Engines. 75*s.* (76*s.* 8*d.*)
Vol. II. Noise, Parachutes, Stability and Control, Structures, Vibration, Wind Tunnels. 47*s.* 6*d.* (49*s.* 2*d.*)

1943 Vol. I. Aerodynamics, Aerofoils, Airscrews. 80*s.* (81*s.* 8*d.*)
Vol. II. Engines, Flutter, Materials, Parachutes, Performance, Stability and Control, Structures. 90*s.* (91*s.* 11*d.*)

1944 Vol. I. Aero and Hydrodynamics, Aerofoils, Aircraft, Airscrews, Controls. 84*s.* (86*s.* 9*d.*)
Vol. II. Flutter and Vibration, Materials, Miscellaneous, Navigation, Parachutes, Performance, Plates and Panels, Stability, Structures, Test Equipment, Wind Tunnels. 84*s.* (86*s.* 9*d.*)

ANNUAL REPORTS OF THE AERONAUTICAL RESEARCH COUNCIL—

1933–34	1*s.* 6*d.* (1*s.* 8½*d.*)	1937	2*s.* (2*s.* 2½*d.*)
1934–35	1*s.* 6*d.* (1*s.* 8½*d.*)	1938	1*s.* 6*d.* (1*s.* 8½*d.*)
April 1, 1935 to Dec. 31, 1936	4*s.* (4*s.* 5½*d.*)	1939–48	3*s.* (3*s.* 3½*d.*)

INDEX TO ALL REPORTS AND MEMORANDA PUBLISHED IN THE ANNUAL TECHNICAL REPORTS, AND SEPARATELY—

April, 1950 - - - - - -	R. & M. No. 2600.	2*s.* 6*d.* (2*s.* 7½*d.*)

AUTHOR INDEX TO ALL REPORTS AND MEMORANDA OF THE AERONAUTICAL RESEARCH COUNCIL—

1909–January, 1954 - - - -	R. & M. No. 2570.	15*s.* (15*s.* 5½*d.*)

INDEXES TO THE TECHNICAL REPORTS OF THE AERONAUTICAL RESEARCH COUNCIL—

December 1, 1936 — June 30, 1939.	R. & M. No. 1850.	1*s.* 3*d.* (1*s.* 4½*d.*)
July 1, 1939 — June 30, 1945. -	R. & M. No. 1950.	1*s.* (1*s.* 1½*d.*)
July 1, 1945 — June 30, 1946. -	R. & M. No. 2050.	1*s.* (1*s.* 1½*d.*)
July 1, 1946 — December 31, 1946.	R. & M. No. 2150.	1*s.* 3*d.* (1*s.* 4½*d.*)
January 1, 1947 — June 30, 1947. -	R. & M. No. 2250.	1*s.* 3*d.* (1*s.* 4½*d.*)

PUBLISHED REPORTS AND MEMORANDA OF THE AERONAUTICAL RESEARCH COUNCIL—

Between Nos. 2251–2349. - -	R. & M. No. 2350.	1*s.* 9*d.* (1*s.* 10½*d.*)
Between Nos. 2351–2449. - -	R. & M. No. 2450.	2*s.* (2*s.* 1½*d.*)
Between Nos. 2451–2549. - -	R. & M. No. 2550.	2*s.* 6*d.* (2*s.* 7½*d.*)
Between Nos. 2551–2649. - -	R. & M. No. 2650.	2*s.* 6*d.* (2*s.* 7½*d.*)

Prices in brackets include postage

HER MAJESTY'S STATIONERY OFFICE

York House, Kingsway, London W.C.2; 423 Oxford Street, London W.1 (Post Orders: P.O. Box 569, London S.E.1); 13a Castle Street, Edinburgh 2; 39 King Street, Manchester 2; 2 Edmund Street, Birmingham 3; 109 St. Mary Street, Cardiff; Tower Lane, Bristol 1; 80 Chichester Street, Belfast, *or through any bookseller*

S.O. Code No. 23-2935

R. & M. No. 2935